



Signe Šetlere

ORCID 0000-0003-1983-6169

Neurofilament Light Chain and
Metabolome as Biomarkers of
Disease Severity and Progression in
Charcot-Marie-Tooth Disease

Summary of the Doctoral Thesis for obtaining
the scientific degree “Doctor of Science (*PhD*)”

Sector Group – Medical and Health Sciences

Sector – Clinical Medicine

Sub-Sector – Neurology

Rīga, 2025

The Doctoral Thesis was developed at Rīga Stradiņš University, Latvia

Supervisor of the Doctoral Thesis:

Dr. med., Assistant Professor **Viktorija Kēniņa**,
Rīga Stradiņš University, Latvia

Scientific Advisor:

Dr. chem., Assistant Professor **Kristaps Kļaviņš**,
Rīga Technical University, Latvia

Official Reviewers:

Dr. med., Professor **Guntis Karelis**,
Rīga Stradiņš University, Latvia

PhD, Associate Professor **Liis Väli**,
University of Tartu, Estonia

PhD, Associate Professor **Antanas Vaitkus**,
Lithuanian University of Health Sciences

Defence of the Doctoral Thesis will take place at the public session of the Promotion Council of Clinical Medicine on 16 December 2025 at 15.00 in the 3rd Auditorium, 16 Dzirciema Street, Rīga Stradiņš University

The Doctoral Thesis is available in RSU Library and on RSU website:
<https://www.rsu.lv/en/dissertations>



Participation in THE FLPP project
“Research of biomarkers of Charcot-Marie-Tooth neuropathy
progression and Clinical diversity”
No. IzP-2021/1-0327

Secretary of the Promotion Council:

Dr. med., Professor **Juta Kroiča**

Table of Contents

Abbreviations used in the Thesis	5
Introduction	6
Aim of the Thesis	7
Objectives of the Thesis	7
Hypotheses of the Thesis	8
Novelty of the Thesis	8
Personal Contribution	10
1 Materials and methods	11
1.1 Ethical considerations of the study	11
1.2 Inclusion of study participants in the study	11
1.3 Characterisation and evaluation of study participants	12
1.4 Blood sample collection and testing procedures	14
1.4.1 Genetic testing	14
1.4.2 Neurofilament light chain concentration measurement	17
1.4.3 Metabolomics	17
1.5 Statistical analysis	18
2 Results	20
2.1 Characterisation of the CMT Patient Cohort	20
2.2 Genetic Characterisation of the CMT Patients	20
2.3 Plasma Neurofilament Light Chain (NfL) Concentration and Disease Severity Assessment	22
2.4 Follow-up Evaluation of CMT Patients After 3 Years	24
2.4.1 Paediatric CMT patients	28
2.5 Metabolome	29
2.5.1 Predictive abilities of CMT-related biomarkers	32
2.5.2 Metabolic profiles in CMT of different severity	33
Discussion	36
Neurofilament light chain concentration in plasma as a biomarker of CMT progression	39
Plasma metabolites as biomarkers of CMT	43
Study limitations	50
Conclusions	51
Proposals	52
List of publications	53
References	54

Acknowledgements 62

Annexes 63

 Annex 1 64

 Annex 2 65

 Annex 3 67

 Annex 4 68

Abbreviations used in the Thesis

ACMG	American College of Medical Genetics and Genomics
CMAP	compound muscle action potential
CMT	Charcot-Marie-Tooth disease
CMTNSv2	Charcot-Marie-Tooth Neuropathy Score version 2
EDTA	ethylenediaminetetraacetic acid
<i>GJB1</i>	Gap Junction Protein Beta 1 gene
<i>HINT1</i>	histidine triad nucleotide-binding protein 1
HNPP	hereditary neuropathy with liability to pressure palsies
<i>HSPB1</i>	heat shock protein beta-1 gene
LC–MS	liquid chromatography–mass spectrometry
<i>MFN2</i>	mitofusin 2 gene
MLPA	multiplex ligation-dependent probe amplification
<i>MPZ</i>	myelin protein zero gene
MRC	Medical Research Council
MS	mass spectrometry
m/z	mass-to-charge ratio
NF	neurofilament
NfL	neurofilament light chain
NMAN	neuromyotonia and axonal neuropathy
<i>PMP22</i>	peripheral myelin protein 22 gene
Simoa	single molecule array
VUS	variant of unknown significance

Introduction

Charcot-Marie-Tooth (CMT) disease is a motor and sensory neuropathy characterised by marked clinical and genetic heterogeneity. It is the most common inherited neuromuscular disorder, with an estimated prevalence of approximately 1 in 2500 individuals.(Eggermann et al., 2018). Currently, no disease-specific treatment is available for Charcot-Marie-Tooth (CMT) disease. CMT is a slowly progressive neuropathy; therefore, the evaluation of disease progression within the relatively short duration of clinical trials requires reliable biomarkers that reflect the underlying pathophysiological changes. To date, various clinical and molecular candidate biomarkers have been investigated for this purpose (Dortch et al., 2014; Ebenezer et al., 2007; Fledrich et al., 2017; Millere et al., 2021; Morrow et al., 2018; Morrow et al., 2016; Murphy et al., 2011; Sames et al., 2014; Sandelius et al., 2018; Shy et al., 2005). Although the number of studies continues to increase, no biomarker has yet been identified that reliably reflects the relatively slow progression of the disease and could be used to assess disease severity and progression. Currently, two promising candidate biomarkers are under consideration: plasma levels of neurofilament light chain (NfL) as an indicator of axonal damage, and muscle magnetic resonance imaging (MRI) for evaluating the degree of muscle atrophy. (Cornett et al., 2019; Millere et al., 2021; Rossor et al., 2020; Sandelius et al., 2018).

Neurofilaments are cytoskeletal proteins found in both the central and peripheral nervous systems, where they contribute to the structural integrity and morphology of neurons. They are particularly abundant in neuronal axons. It is well established that axonal injury leads to the release of neurofilaments, including neurofilament light chain (NfL), into the bloodstream. Therefore, plasma NfL concentration is considered a promising biomarker for disorders characterised by axonal degeneration (Khalil et al., 2020; Khalil et al., 2018; Yuan et al., 2017). To date, studies have reported a correlation between plasma

NfL levels and disease severity in Charcot-Marie-Tooth (CMT) disease (Millere et al., 2021; Sandelius et al., 2018). However, it remains unclear whether plasma NfL levels are associated with disease progression.

Metabolomic analysis, which involves quantifying various metabolites in blood, is an effective approach for identifying novel biomarkers. By comparing the metabolomic profiles of patients with neuropathy to those of healthy individuals, it is possible to detect specific differences that may subsequently be utilised for diagnostic purposes, prognostic evaluation, and assessment of therapeutic efficacy. To date, several studies have demonstrated associations between specific metabolites and the development of diabetic polyneuropathy. (Akbar et al., 2017; Hsu et al., 2012; Hwang et al., 2016; Shao et al., 2022; Zhao et al., 2015; Zhu et al., 2011). In a cohort of 42 individuals with CMT1A, twelve serum metabolites were identified as candidate biomarkers, suggesting their potential utility in disease monitoring (Soldevilla et al., 2017). However, the results of previously published studies have not been validated, and data on the biomarker potential of metabolomic profiles in the group of inherited neuropathies remain limited.

Aim of the Thesis

To evaluate changes in plasma NfL levels and metabolite biomarkers in patients with CMT and to analyse their association with clinical disease severity, genetic subtypes, and disease progression.

Objectives of the Thesis

- 1 To perform longitudinal clinical and electrophysiological evaluation of a previously established cohort of Charcot-Marie-Tooth patients, with follow-up assessment conducted after a 3-year interval.
- 2 To determine plasma NfL concentrations in patients with Charcot-Marie-Tooth disease and in a control group, and to analyse

their association with clinical disease severity across different CMT subtypes.

- 3 To assess the association between changes in NfL levels over a 3-year period and clinical disease progression in Charcot-Marie-Tooth patients.
- 4 To perform targeted metabolomic analysis in patients with Charcot-Marie-Tooth disease and in a control group, and to analyse metabolomic profiles across different CMT subtypes.
- 5 To evaluate the prognostic value of metabolite concentrations for the classification of CMT subtypes and to assess their association with clinical disease severity.

Hypotheses of the Thesis

- 1 Plasma NfL concentration is associated with clinical disease severity and progression in CMT.
- 2 Blood metabolite biomarker concentrations are associated with the genetic subtype of CMT and the severity of clinical manifestations.

Novelty of the Thesis

CMT patient population is both genetically and clinically heterogeneous. The disease is characterised by a chronic, slowly progressive neuropathy that may affect both motor and sensory nerves. Currently, there is no effective pharmacological treatment available; however, clinical trials aimed at developing such therapies are actively ongoing. Therefore, the identification of biomarkers capable of evaluating treatment efficacy is of particular importance. Ideally, such biomarkers should not only reflect the functional status of the disease but also enable the assessment and prediction of its relatively slow progression.

In peripheral nervous system disorders involving axonal damage or degeneration, plasma NfL levels increase and correlate with disease severity. (Mariotto et al., 2018). A recent study confirmed that plasma NfL levels are significantly elevated in patients with CMT and are associated with disease severity when measured at a single time point. (Millere et al., 2021). In contrast, a longitudinal study did not demonstrate significant changes in plasma NfL levels over a six-year interval (Rossor et al., 2022). Although NfL is a promising biomarker for CMT, current evidence regarding its utility as a marker of disease progression remains inconclusive. This study presents data on changes in NfL levels in a larger patient cohort compared to previously published studies. Furthermore, it evaluates disease progression and the association between NfL levels and disease severity in both adult and paediatric CMT patients.

In recent years, metabolomic analysis has been widely used for the identification of diagnostic and prognostic disease biomarkers. Knowledge of metabolites involved in various metabolic pathways may contribute to a better understanding of disease pathogenesis, as well as to the identification of biomarkers and potential therapeutic targets. Although the metabolome has previously been investigated in patients with peripheral nervous system disorders, no metabolites have yet been identified as effective markers for assessing disease progression in inherited neuropathies. In this study, metabolite levels and their interrelationships were analysed in patients with CMT and compared to a control group. Additionally, metabolomic profiles were examined across genetic subgroups and different levels of disease severity. The associations between candidate metabolite biomarkers and CMT severity were also explored.

To date, no studies in Latvia have investigated dynamic changes in the metabolome or plasma NfL levels in patients with inherited neuropathies. Furthermore, no previously published international studies have reported data on

a CMT patient cohort as large as the one included in this work. The results of this study provide novel insights into potential biomarkers for inherited neuropathies and their practical applicability in the clinical management of CMT.

Personal Contribution

The author planned the study, participated in the selection and clinical evaluation of the study participants. The author has compiled, processed, and analysed the data, including statistical methods. The author prepared scientific publications and wrote this Thesis.

1 Materials and methods

1.1 Ethical considerations of the study

The study was conducted in accordance with the Declaration of Taipei and the Declaration of Helsinki of the World Medical Association, the Convention on Human Rights and Biomedicine (Oviedo Convention), as well as the applicable regulatory acts of the Republic of Latvia. The study protocol was approved by the Central Medical Ethics Committee of Latvia (Approval No 3/18-03-21, Annex 1). All participants were included only after providing written informed consent, confirming that they had been informed about the study's purpose and procedures. In cases where participants were under the age of 18, consent was obtained from their legal or appointed representative.

1.2 Inclusion of study participants in the study

In the patient group with available clinical evaluation and NfL measurements, patients were included from the clinical practices of a geneticist, a neurologist, and a paediatric neurologist at the Children's Clinical University Hospital, as well as from the Center for Neuroimmunology and Immunodeficiencies, comprising a total of 101 patients. Repeated NfL level measurement and clinical evaluation were performed in 73 CMT patients. Meanwhile, metabolomic analysis was carried out in 84 patients.

Inclusion criteria for the patient groups required written informed consent for participation in the study, as confirmed by a signed informed consent form from the patient or their legal representative. To be enrolled in one of the study groups, each participant had to meet at least one of the following criteria:

- 1 Clinical and/or neurophysiological findings consistent with CMT, together with a genetically confirmed diagnosis and/or a positive family history.
- 2 Clinical and neurophysiological findings consistent with CMT.

3 Genetically confirmed diagnosis of CMT.

Exclusion criteria included any known comorbidities of the central or peripheral nervous system that could influence the results or interpretation of NfL or metabolomic analyses, as well as refusal to participate in the study.

The study also included a control group for both NfL concentration and metabolomic analyses. Plasma NfL levels were measured in 64 control participants, repeated measurement of NfL levels in 28 participants, while metabolomic analysis was performed in 34 individuals. The control group was selected to match the patient group in terms of age and sex distribution, and no statistically significant differences in age or sex were observed between the groups.

Control group participants were individuals available to the research team, including medical personnel, healthy relatives of patients (only from families in which the genetically identified pathogenic variant had not been detected in these relatives), as well as other physically accessible individuals without neurological symptoms. No additional neurological examination was performed in control group participants; however, they were required to meet the following inclusion criteria:

- 1 Healthy individual without known neurological diseases or symptoms;
- 2 Written informed consent to participate in the study.

1.3 Characterisation and evaluation of study participants

Patients or their legal representatives completed a sociodemographic questionnaire, providing information on age, sex, age at symptom onset, and the time interval between symptom onset and diagnosis. All patients underwent clinical and neurophysiological evaluation using standardised assessment tools.

Nerve conduction studies were performed in all patients according to a standardised protocol for the diagnosis of polyneuropathy (Novello & Pobre, 2025). All nerve conduction studies were performed by a single specialist using the *Dantec Keypoint Focus EMG/NCS/EP system*. The examination protocol

began with motor nerve conduction studies of the lower limbs, specifically the peroneal (*n. peroneus*) and tibial (*n. tibialis*) nerves, followed by assessment of sensory nerves, including the sural (*n. suralis*) and superficial peroneal (*n. peroneus superficialis*) nerves. Subsequently, the upper limbs were evaluated by analysing both motor and sensory fibres of the ulnar nerve (*n. ulnaris*) and the sensory fibres of the radial nerve (*n. radialis*). In both the lower and upper limbs, side-to-side comparisons were made to assess symmetry. Nerve conduction data were used to classify patients according to CMT subtypes based on motor nerve conduction velocity: demyelinating form (CMT1), axonal form (CMT2), or intermediate/mixed form (Bird, 2025). The obtained data were also used to complete disease-specific clinical rating scales.

To assess the clinical status of patients, a disease-specific severity scale CMTNSv2 (Charcot-Marie-Tooth Neuropathy Score version 2) was used (Murphy et al., 2011), Annex 2. CMTNSv2 is a disease-specific scale that incorporates multiple components to assess the severity of CMT. It includes an evaluation of sensory disturbances, such as the level of sensory loss in the lower limbs, vibratory perception, and pinprick sensation. Motor function is assessed separately for the upper and lower limbs by grading muscle strength according to the Medical Research Council (MRC) scale. The scale also evaluates functional abilities in daily activities and includes neurophysiological data. The neurophysiological section comprises findings from two upper limb nerve conduction study sites: the compound muscle action potential (CMAP) of the ulnar or median nerve, and the sensory nerve action potential (SAP) of the radial nerve. Although CMT most commonly affects the lower limbs, upper limb nerves are used in this scale because lower limb nerves are often severely affected early in the disease course, with little change over time, limiting their usefulness in tracking progression. Each item in the CMTNSv2 is scored from 0 to 4, yielding a total score ranging from 0 to 36. Higher scores indicate

greater disease severity. The total score is often interpreted categorically as follows: mild (0–10 points), moderate (11–20 points), and severe (21–36 points) disease (Murphy et al., 2011).

1.4 Blood sample collection and testing procedures

Blood sample collection and storage were carried out in accordance with a strict standard operating procedure. Following an outpatient visit, certified medical personnel collected two to three EDTA-containing (ethylenediaminetetraacetic acid containing) blood tubes from each patient for the purposes of plasma NfL measurement, genetic subtype confirmation (for patients without a previously confirmed genetic diagnosis), and metabolomic analysis. Two EDTA tubes were collected from each control group participant for NfL and metabolomic analyses. All blood samples were processed within one hour. For NfL measurement, one EDTA tube was centrifuged at room temperature for 10 minutes at 3500 rpm. The resulting plasma was aliquoted and stored at -20°C . The second EDTA tube was stored at $+4^{\circ}\text{C}$ and, if needed, transported to the RSU Molecular Genetics Research Laboratory within one week for DNA extraction.

1.4.1 Genetic testing

Two methods were used for DNA extraction: a commercially available kit (*Analytik Jena, Germany*) and a modified phenol–chloroform protocol. Both methods were applied to isolate DNA from peripheral blood samples collected from participants in the patient group (Rovite et al., 2018).

PMP22 gene copy number determination

DNA quality was assessed quantitatively using a Nanodrop UV/VIS spectrophotometer (*ThermoFisher Scientific, USA*). The first step of genetic testing involved the determination of *PMP22* gene copy number using

the multiplex ligation-dependent probe amplification (MLPA) kit P405 (*MRC Holland, Netherlands*). This reagent kit simultaneously assesses copy number variations in the *PMP22*, *GJB1*, and *MPZ* genes. The reaction mix contains 42 MLPA probes, with amplification products ranging in size from 130 to 445 nucleotides. Of these, 17 probes target the 17p12 region, two probes cover the flanking region, seven probes target the *MPZ* gene, and five probes target the *GJB1* gene. In addition, 10 reference probes for various autosomal regions and three probes for the X chromosome are included. The assay was performed according to the manufacturer's protocol. Following the reaction, 1 µl of each sample was mixed with 12 µl of Hi-Di formamide and 0.5 µl of the GeneScan LIZ500 size standard (*Thermo Fisher Scientific, USA*), and the mixture was subjected to capillary electrophoresis using the ABI 3500 Genetic Analyzer (*Thermo Fisher Scientific, USA*). Data analysis was performed using Coffalyser software in accordance with the manufacturer's recommendations. Control DNA samples with known *PMP22* copy numbers were used for validation. A fluorescent signal ratio between 0.7 and 1.3 was interpreted as normal (two gene copies), a ratio below 0.7 indicated a deletion, and a ratio above 1.3 indicated a duplication.

***GJB1* gene determination**

In patients with clinical features or a family history suggestive of the CMTX1 subtype, as well as in those with normal *PMP22* gene copy numbers, bidirectional Sanger sequencing of the *GJB1* gene exons and exon–intron boundaries was performed. Sequencing was carried out using the BigDye Terminator v3.1 Cycle Sequencing Kit (*ThermoFisher Scientific, USA*), following a modified version of the manufacturer's protocol. The purification of PCR products was conducted using exonuclease I and shrimp alkaline phosphatase (SAP), followed by ethanol and EDTA precipitation prior to capillary electrophoresis (Kovale et al., 2021).

Analysis of sequencing electropherograms was performed using Chromas 2.6.6 software (<http://technelysium.com.au/wp/chromas/>). The obtained sequences were aligned and compared with reference sequences available in the Nucleotide BLAST database: NG_008357.1 and NM_000166.6 (BLAST: *Basic Local Alignment Search Tool*, n.d.).

Exome sequencing

For patients with negative results from previous genetic testing, exome sequencing was performed. The analysis was carried out in accordance with ISO 15189 standards at CeGaT, an accredited medical laboratory in Germany, using reagents from Twist Bioscience (*Twist Bioscience, USA*). The resulting data were analysed at the RSU Molecular Genetics Scientific Laboratory (MGZL) using a laboratory-developed bioinformatic pipeline capable of detecting single nucleotide variants (SNVs), small insertions and deletions (indels), and copy number variations (CNVs). The bioinformatics algorithm was validated using reference samples with known genotypes, including those with microsatellite repeat expansions and exon-level duplications or deletions. Identified genetic variants were annotated using the Illumina Variant Interpreter platform (*Illumina, USA*). The exome sequencing analysis specifically targeted genes associated with neuropathy (Appendix 3). Gene selection was based on publicly available resources, including PanelApp (<http://panelapp.genomicsengland.co.uk/#/>), Blueprint laboratory data, and relevant scientific literature.

Identified genetic variants were interpreted and classified according to the guidelines of the American College of Medical Genetics and Genomics (ACMG) into the following categories: benign, likely benign, variants of uncertain significance (VUS), likely pathogenic, and pathogenic. (Richards et al., 2015). Pathogenic and likely pathogenic variants, as well as selected variants of uncertain significance (VUS), were confirmed by bidirectional Sanger

sequencing in the index patient and, when consent was obtained, also in family members who agreed to participate in the study.

1.4.2 Neurofilament light chain concentration measurement

NfL analyses were performed at the Institute of Neuroscience and Physiology, Sahlgrenska Academy, University of Gothenburg. The time between blood collection and NfL analysis was 3–4 months, during which plasma samples were stored at -20°C . Plasma NfL concentrations were measured using a single molecule array (*Simoa*) NfL assay (*Quanterix, USA*).

Samples were analysed blinded to case – control status and in randomised order. Each sample was diluted fourfold and processed individually, with results interpreted accordingly based on the dilution factor. The dynamic range of the assay was 1.9–1800 pg/mL.

1.4.3 Metabolomics

Plasma metabolomic analysis was performed using ultra-high-performance liquid chromatography coupled with mass spectrometry (UHPLC–MS). A panel of 33 metabolites was quantified in plasma samples from both CMT patients and healthy controls (Appendix 4). These specific metabolites were selected based on the availability of corresponding analytical standards and isotopically labelled internal standards, which are essential for accurate quantitative analysis. Additionally, the chosen metabolites were selected because the majority are routinely measured by mass spectrometry as part of newborn screening programs (Lehotay et al., 2011). Thus, by measuring these already well-characterised markers, the observed alterations in the blood of CMT patients may serve as a readily implementable diagnostic tool for the identification of this disease in clinical practice.

LC–MS analysis was performed using the Dionex 3000 HPLC liquid chromatography system (*Thermo Fisher Scientific, USA*), coupled to an *Orbitrap*

Q Exactive mass spectrometer (Thermo Fisher Scientific, USA). Chromatographic separation was achieved using an *ACQUITY UPLC BEH Amide* column (1.7 μm , 2.1×100 mm; Waters, USA) with a *VanGuard BEH C18* guard column (2.1×5 mm; Waters, USA). The column temperature was maintained at 40 °C, and the injection volume was 2 μL . The mobile phases consisted of phase A: water with 0.15 % formic acid and 10 mM ammonium formate, and phase B: 85 % acetonitrile with 0.1 % formic acid and 10 mM ammonium formate. Gradient elution was performed at a flow rate of 0.4 mL/min, with a total run time of 17 minutes. The *Orbitrap Q Exactive mass spectrometer* was operated in positive electrospray ionisation (ESI) mode with the following parameters: spray voltage 3.5 kV, vaporiser temperature 400 °C, capillary temperature 350 °C, auxiliary gas flow 12, and sheath gas flow 50. Full scan MS data were acquired over an m/z range of 50–400 with a resolution of 35 000, an AGC target of 1×10^6 , and a maximum injection time of 50 ms.

Data were processed using TraceFinder 4.1 software (Thermo Fisher Scientific, USA). The method included defined retention times and m/z values for each analyte. Ion signal spectra generated by the mass spectrometer were interpreted in the software to generate chromatograms for each analyte. Peak areas were identified and quantified based on calibration curves constructed from standard solutions with known concentrations. Analyte concentrations were calculated using the corresponding peak areas, assuming a linear relationship between peak area and concentration. Quantification was performed using a seven-point linear calibration curve with internal standardisation and $1/\times$ weighting.

1.5 Statistical analysis

All statistical analyses were performed using IBM SPSS Statistics (version 27.0), *Prism 9*, and *MetaboAnalyst 6.0* (www.metaboanalyst.ca). The normality of continuous variables was assessed using histograms, Q–Q

plots, and the Shapiro–Wilk test. For normally distributed data, group comparisons were performed using the t-test. For non-normally distributed data, the Mann–Whitney U test was applied. Categorical variables were compared using Pearson’s chi-square test. Correlations between continuous variables were analysed using Spearman’s rank correlation coefficient.

Metabolite concentrations were normalised to the sample matrix to reduce the influence of inter-assay variability across measurement batches. By default, metabolites with more than 20 % missing values were excluded from the analysis; however, in this dataset, such exclusion was not necessary. Fold changes (FC) and p-values were visualised using volcano plots, with thresholds for significance set at $FC > 1.3$ and $p < 0.05$. These plots were generated using *Prism 9* software. Normalised concentrations were visualised using violin plots, and statistical significance was assessed using Sidak’s multiple comparisons test. Orthogonal partial least squares discriminant analysis (OPLS-DA) was performed using MetaboAnalyst 6.0. Prior to analysis, the data were log10-transformed and scaled by mean-centring and dividing by the square root of the standard deviation (Pareto scaling) for each metabolite.

Multivariate regression analysis was used for the development of predictive models, and group classification was performed using a linear support vector machine (SVM) algorithm. The importance of individual metabolites within these models was evaluated using the Random Forest method. Receiver operating characteristic (ROC) curves were used to determine optimal classification thresholds, and the quality of these thresholds was assessed by calculating the area under the curve (AUC).

2 Results

2.1 Characterisation of the CMT Patient Cohort

Data on the CMT cohort have been previously published in the study by Millere et al. (Millere et al., 2021) In addition, this study included five new CMT patients and four healthy control participants, resulting in a total cohort of 101 CMT patients and 64 healthy individuals. The patient group comprised individuals from 72 distinct families. The mean age of the CMT patients was 37.8 ± 18.0 years, and the sex distribution was 46 males and 55 females.

2.2 Genetic Characterisation of the CMT Patients

CMT patients were stratified according to their genetic subtype. Duplication of the *PMP22* gene was identified in 44 patients, while disease-causing variants in the *GJB1* gene were found in 14 patients. Pathogenic variants in the *MFN2* gene were detected in 4 patients, and *PMP22* gene deletions were observed in 3 patients. Additionally, pathogenic variants in the *HINT1* gene were identified in 6 patients. Other disease-causing variants were found in the following genes: *HSPB1* (n = 2), *AARS1* (n = 2), *BSC12* (n = 1), *MPZ* (n = 1), *MORC2* (n = 1), and *BICD2* (n = 1). The gene variants were listed in the ClinVar database and known as (likely) pathogenic.

In the patient group, exome sequencing identified two previously unreported variants in the *AARS1* gene (reference transcript ENST00000261772.12) in two patients – c.1823C>A p.(Thr608Lys) and c.1815C>G p.(His605Gln). Both variants were initially classified as VUS according to ACMG guidelines, and the following criteria were applied: the variants had not been previously reported either in population databases (gnomAD and TOPMED) (PM2) or in the literature in patients with peripheral neuropathies; they are located in the *AARS1* editing domain, where other pathogenic missense variants have been described (Zhang et al., 2021) (PM1);

furthermore, only missense variants in the heterozygous state have been reported as pathogenic in CMT2N; the codon amino acid is conserved across species, and multiple *in silico* prediction tools suggest a pathogenic effect on the protein (PP3). Segregation of the variant within the family is essential for determining its pathogenicity. Testing of family members was performed: for variant c.1823C>A p.(Thr608Lys), two symptomatic and three healthy individuals were examined; for variant c.1815C>G p.(His605Gln), three symptomatic family members were examined. For both variants, this allowed application of the PP1 Supporting criterion (Figure 2.1). Since the variants segregated with the symptomatic family members, they were classified as pathogenic, providing molecular confirmation of the disease.

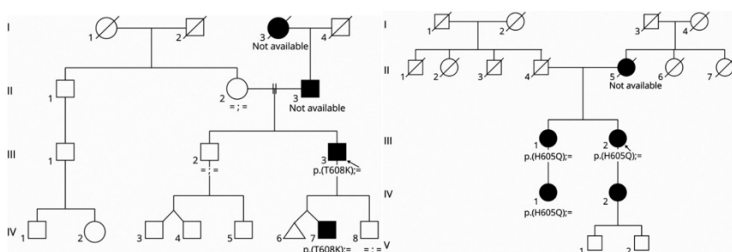


**Figure 2.1 Segregation analysis of AARS1 gene variants
ENST00000261772.12: c.1823C>A p.(Thr608Lys) and
c.1815C>G p.(His605Gln)**

=/= – variant not identified

Both patients presented with lower limb weakness, pain and tingling sensations in the legs, foot deformities (*pes cavus*), and general fatigue. Electrophysiological examination in both cases revealed axonal demyelinating sensorimotor neuropathy, with nerve conduction velocities consistent with an intermediate form of CMT. The CMTNSv2 scores for the two patients were 5 and 14, respectively.

2.3 Plasma Neurofilament Light Chain (NfL) Concentration and Disease Severity Assessment

As previously demonstrated in the publication by Millere et al. (Millere et al., 2021), plasma NfL concentrations were elevated in the present CMT cohort (median = 12.5 pg/mL, IQR = 7.5 pg/mL) compared to the control group (median = 5.2 pg/mL, IQR = 3.0 pg/mL). This difference was statistically significant (Mann–Whitney U test, $U = 749.000$, $p < 0.001$). The distribution of NfL concentrations across study groups is shown in Figure 2.2.

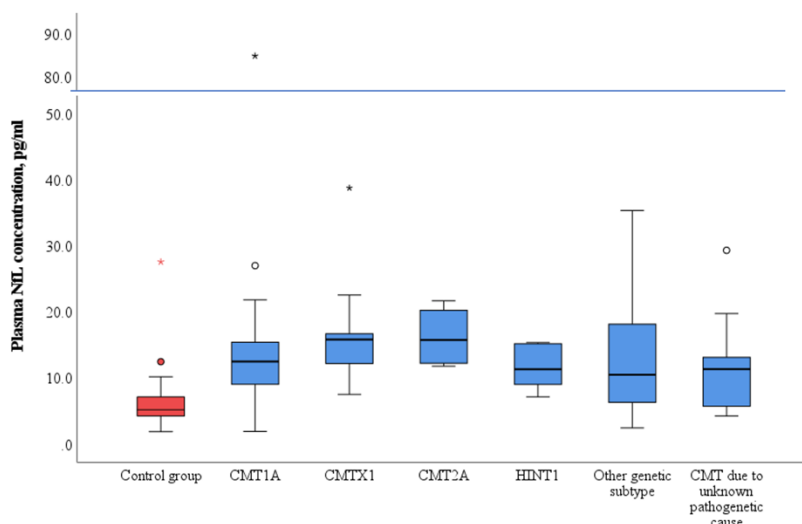


Figure 2.2 Plasma NfL concentrations in different study groups

Disease severity was assessed using the CMTNSv2 scale. The relationship between disease severity and the genetically defined CMT subtypes was subsequently evaluated. No significant differences in severity were observed between the different genetic groups (Kruskal–Wallis H test, $H = 8.633$, $p = 0.195$). The median CMTNSv2 scores and interquartile ranges for each group are presented in Table 2.1.

Table 2.1

NfL and CMTNSv2 across study groups

Study participants	Number of patients (male/female)	Mean age (SD)	Median NfL, pg/mL (IQR)	Median CMTNSv2 (IQR)	CMTNSv2/NfL Spearman correlation coefficient
All CMT patients	101 (46/55)	37.8 (± 18.0)	12.5 (7.5)	10.0 (11.0)	0.284, p = 0.004
CMT1A (PMP22 dup)	44 (19/25)	36.2 (± 16.4)	12.5 (6.4)	12.0 (7.0)	0.118, p = 0.444
CMTX1 (GJB1)	14 (6/8)	36.3 (± 19.2)	15.8 (6.1)	12.5 (19.0)	-0.132, p = 0.667
CMT2A (MFN2)	4 (2/3)	32.0 (± 14.9)	15.7 (9.0)	6.5 (15.0)	-0.738, p = 0.262
HNPP (PMP22 del)	3 (1/2)	30.7 (± 18.7)	9.4 (NA)	0.0 (NA)	0.866, p = 0.333
NMAN (HINT1)	6 (2/4)	37.8 (± 24.2)	11.3 (6.7)	11.5 (9.0)	0.986, p < 0.001
CMT2F (HSPB1)	2 (0/2)	46.0 (± 26.9)	14.0 (NA)	10.0 (NA)	NA
CMT2N (AARS1)	2 (1/1)	46.5 (± 13.4)	3.1 (NA)	9.5 (NA)	NA
CMT1E (PMP22 SNV)	1 (1/0)	32.0 (NA)	6.9 (NA)	21.0 (NA)	NA
HMN5C (BSCL2)	1 (1/0)	45.0 (NA)	11.5 (NA)	2.0 (NA)	NA
CMT2I (MPZ)	1 (0/1)	63.0 (NA)	35.4 (NA)	20.0 (NA)	NA
CMT2Z (MORC2)	1 (1/0)	46.0 (NA)	14.9 (NA)	7.0 (NA)	NA
SMALED2A (BICD2)	1 (0/1)	43.0	21.4 (NA)	17.0 (NA)	NA
CMT with unknown monogenic cause	21 (12/9)	40.9 (± 23.8)	11.3 (8.8)	5.0 (8.0)	0.631, p = 0.002
Control group	64 (22/42)	34.8 (± 12.1)	5.2 (3.0)	NA	NA

CMT – Charcot-Marie-Tooth disease; NfL – neurofilament light chain; IQR – interquartile range, CMTNSv2 – CMT Neuropathy Score v.2; NA – not applicable; dup – duplication; del – deletion; SNV – single nucleotide variant

To evaluate the relationship between NfL concentration and disease severity, the correlation with the CMTNSv2 score was analysed. In the overall CMT cohort, plasma NfL concentration showed a statistically significant but weak correlation with CMTNSv2 (Spearman's correlation, $r = 0.284$, $p = 0.004$) (Figure 2.3). A statistically significant and strong correlation was observed within the *HINT1* genetic subgroup (Spearman's correlation, $r = 0.986$, $p < 0.001$) (Table 2.1).

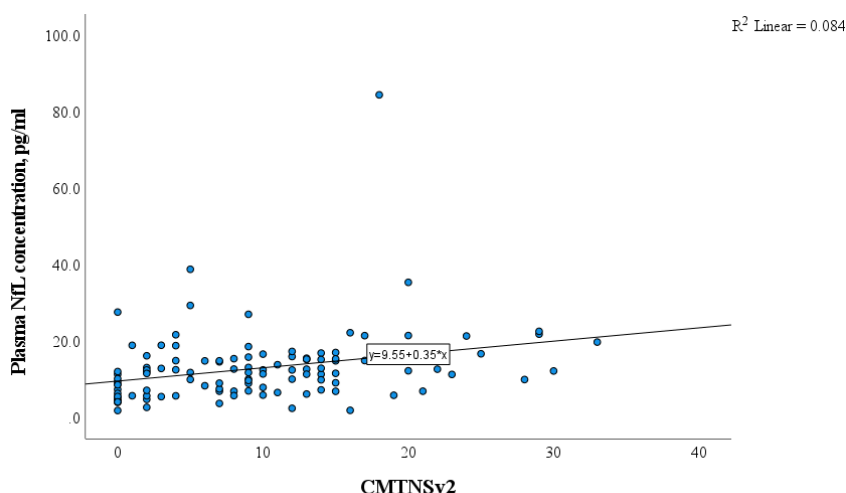


Figure 2.3 Correlation between plasma NfL concentration and CMTNSv2

2.4 Follow-up Evaluation of CMT Patients After 3 Years

Follow-up clinical evaluation and blood sample testing were performed for 73 CMT patients and 28 control group participants (Table 2.2).

To assess disease progression, the CMTNSv2 score was re-evaluated after three years. At follow-up, the score was slightly higher than at baseline (median change = 1.0, IQR = 3.0; Wilcoxon signed-rank test: $Z = -5.673$, $p < 0.001$). Notably, no CMT patient showed a decrease in the CMTNSv2 score during this period.

Table 2.2

Three-year follow-up data of plasma NfL concentration and CMTNSv2 in CMT

Study participants	Number of patients	Mean age (SD)	Median baseline NfL, pg/mL (IQR)	Median follow-up NfL, pg/mL (IQR)	Median change in NfL, pg/mL (IQR)	Median baseline CMTNSv2 (IQR)	Median follow-up CMTNSv2 (IQR)	Median change in CMTNSv2 (IQR)	Changes in CMTNSv2/ changes in NfL Spearman correlation coefficient
All CMT patients	73	38.0 (± 16.4)	12.6 (6.8)	14.6 (7.5)	1.6 (4.4)	11.0 (9.0)	13.0 (8.0)	1.0 (3.0)	0.225, p = 0.054
CMT1A (PMP22 dup)	37	36.2 (± 16.5)	12.5 (6.7)	14.8 (7.5)	2.3 (4.1)	11.0 (7.0)	13.0 (6.0)	1.0 (3.0)	0.302, p = 0.069
CMTX1 (GJB1)	12	37.9 (± 19.2)	16.0 (6.2)	16.4 (15.2)	1.3 (11.6)	17.0 (19.0)	21.0 (16.0)	2.0 (4.8)	-0.29, p = 0.929
CMT2A (MFN2)	4	28.2 (± 14.9)	15.7 (9.0)	14.4 (10.0)	-1.0 (6.3)	6.5 (15.5)	6.5 (15.0)	0.0 (0.0)	NA
CMT2F (HSPB1)	1	65.0 (NA)	22.2 (NA)	21.1 (NA)	-1.1 (NA)	16.0 (NA)	16.0 (NA)	0.0 (NA)	NA
NMAN (HINT1)	5	42.6 (± 23.7)	12.9 (7.2)	15.8 (5.8)	4.6 (2.3)	14.0 (10.0)	14.0 (10.0)	2.0 (3.0)	0.527, p = 0.362
CMT2N (AARS1)	2	46.5 (± 13.4)	3.1 (NA)	4.3 (NA)	1.2 (NA)	9.5 (NA)	10.5 (NA)	1.0 (NA)	NA
CMT1E (PMP22 SNV)	1	32.0 (NA)	6.9 (NA)	10.9 (NA)	4.0 (NA)	21.0 (NA)	27.0 (NA)	6.0 (NA)	NA
HMN5C (BSCL2)	1	45.0 (NA)	11.5 (NA)	9.2 (NA)	-2.3 (NA)	2.0 (NA)	6.0 (NA)	4.0 (NA)	NA

Table 2.2 continued

Study participants	Number of patients	Mean age (SD)	Median baseline NFL, pg/mL (IQR)	Median follow-up NFL, pg/mL (IQR)	Median change in NFL, pg/mL (IQR)	Median baseline CMTNSv2 (IQR)	Median follow-up CMTNSv2 (IQR)	Median change in CMTNSv2 (IQR)	Changes in CMTNSv2/ changes in NFL Spearman correlation coefficient
CMT2I (MPZ)	1	63.0 (NA)	35.4 (NA)	60.0 (NA)	24.6 (NA)	20.0 (NA)	23.0 (NA)	3.0 (NA)	NA
CMT2Z (MORC2)	1	46.0 (NA)	14.9 (NA)	15.3 (NA)	0.4 (NA)	7.0 (NA)	11.0 (NA)	4.0 (NA)	NA
SMALED2A (BICD2)	1	43.0	21.4 (NA)	7.4 (NA)	-14.0 (NA)	17.0 (NA)	17.0 (NA)	0.0 (NA)	NA
CMT with unknown monogenic cause	7	36.6 (± 12.5)	10.0 (5.6)	7.8 (7.5)	-1.0 (2.36)	8.0 (8.0)	9.0 (11.0)	1.0 (1.0)	0.270, p = 0.588
Control group	28	37.8 (± 11.5)	5.2 (3.3)	5.8 (3.8)	0.6 (1.1)	NA	NA	NA	NA

CMT – Charcot-Marie-Tooth disease; NFL – neurofilament light chain; IQR – interquartile range; CMTNSv2 – CMT Neuropathy Score v.2; NA – not applicable; dup – duplication; del – deletion; SNV – single nucleotide variant

Similar to the baseline analysis, plasma NfL levels at the three-year follow-up remained elevated in the CMT group (median = 14.6 pg/mL, IQR = 7.5 pg/mL) compared to the control group (median = 5.8 pg/mL, IQR = 3.8 pg/mL) (Mann–Whitney U test, $U = 193.500$, $p < 0.001$). Over the three-year period, NfL levels increased in both the CMT group (median change = 1.6 pg/mL, IQR = 4.4 pg/mL) and the control group (median change = 0.6 pg/mL, IQR = 1.1 pg/mL). These changes were statistically significant (paired samples t-test for CMT patients: $t(72) = -2.565$, $p = 0.012$; Wilcoxon signed-rank test for the control group: $Z = -3.325$, $p = 0.001$) (Table 2.2).

Over the three-year period, a decrease in plasma NfL levels was observed in seven control group participants and 22 CMT patients. Among the CMT patients, the decrease was noted in 11 individuals with CMT1A, 4 with CMTX1, 1 with CMT2A, 1 with CMT2F, 2 with other genetic subtypes, and 3 with an unknown genetic aetiology.

Analysis of the relationship between changes in plasma NfL concentration over the three-year period and changes in disease severity revealed no significant correlation within the overall CMT group (Spearman's correlation, $r = 0.228$, $p = 0.052$), nor within the individual CMT subgroups (Figure 2.4).

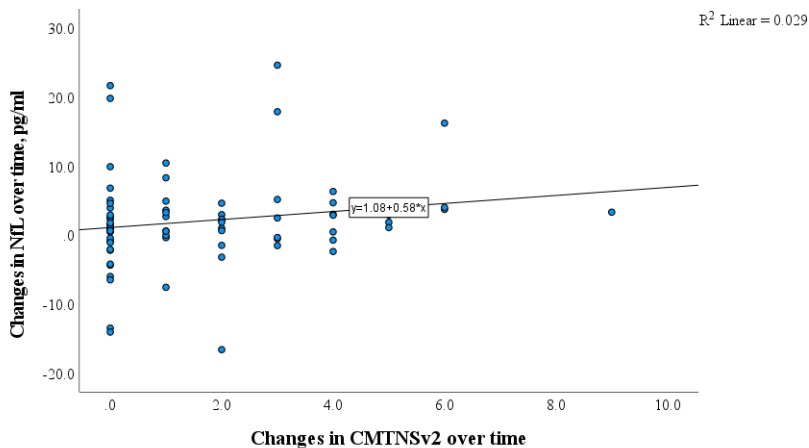


Figure 2.4 **Correlation between plasma NfL concentration and disease severity over a 3-year period in CMT patients**

2.4.1 Paediatric CMT patients

In this study, 19 out of 101 CMT patients were children. In addition to the main cohort analysis, the paediatric subgroup was analysed separately. The genetic distribution among paediatric patients was as follows: CMT1A in 7 patients, CMTX1 in 2, CMT2A in 1, HNPP in 1, and HINT1 in 2 patients. Five children (26 %) had an unknown genetic aetiology, and one patient had not undergone genetic testing. Follow-up evaluation after three years was available for 11 paediatric patients. A median decrease in plasma NfL concentration was observed in the paediatric CMT group (-1.1 pg/mL, IQR = 4.4). The median disease severity score (CMTNSv2) remained unchanged at follow-up (median change = 0.0, IQR = 0), with the exception of one child with biallelic *HINT1* gene mutations, in whom the CMTNSv2 score increased by 4 points. To assess the relationship between changes in plasma NfL levels and changes in CMTNSv2 scores, a correlation analysis was performed, revealing

a weak, statistically non-significant correlation (Spearman's correlation, $r = 0.256$, $p = 0.447$).

2.5 Metabolome

This part of the study included 84 CMT patients and 34 healthy control participants. The patient cohort was stratified according to genetic subtype: CMT1A ($n = 37$), CMTX1 ($n = 17$), CMT2A ($n = 4$), HINT1 ($n = 5$), other genetic types ($n = 14$), and unknown genetic aetiology ($n = 7$).

A total of 33 plasma metabolites were analysed in the CMT patient and control groups (Annex 4). Initial comparisons focused on identifying differential metabolites between the CMT1A ($n = 37$), CMTX1 ($n = 17$), and control groups. The discriminative metabolites were visualised using volcano plots (V-plots) and orthogonal partial least squares discriminant analysis (OPLS-DA) (Figure 2.5 (a–d)). Significant differences were observed in metabolite levels, with elevated acetylcarnitine in the CMT1A group and altered levels of glycine and valine in the CMTX1 group compared to controls ($p < 0.05$, $VIP > 1$, and $FC > 1.3$) (Figure 2.5 (e); Tables 2.3 and 2.4).

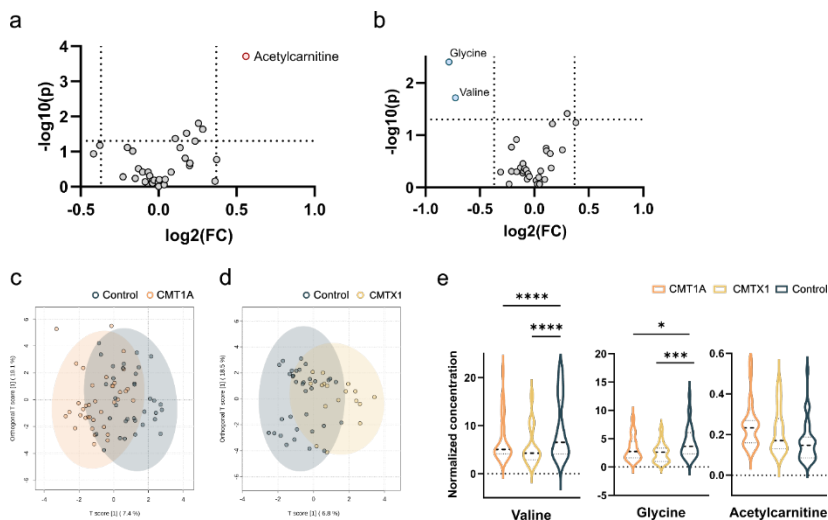


Figure 2.5 Visualisation of differential metabolite profiles compared to healthy controls of a. CMT1A and b. CMTX1 using V-plots

Significance thresholds are indicated with dashed lines ($FC > 1.3$, $p < 0.05$). OPLS-DA plots of c. CMT1A and d. CMTX1. e. Violin plots of metabolites identified to be significantly changed in the volcano plots (**** $p < 0.0001$, ** $p < 0.01$, * $p < 0.05$).

Table 2.3

Differential plasma metabolites between CMT1A patients and healthy controls

Metabolite	p-value	VIP	FC	Control group (median [IQR])	CMT1A (median [IQR])
Acetylcarnitine	1.9384E-4	2.4906	1.4742	10.8350 [9.86]	12.1200 [7.75]

Differential metabolites were selected according to $VIP > 1$, $FC > 1.3$, and $p < 0.05$. Values are expressed as medians [IQR]. P-values were calculated from a t-test for continuous variables; VIP, variable influence on projection; CMT, Charcot-Marie-Tooth disease.

Table 2.4

Differential plasma metabolites between CMTX1 patients and healthy controls

Metabolite	p-value	VIP	FC	Control group (median [IQR])	CMTX1 (median [IQR])
Glycine	0.0039756	2.2636	0.58076	299.9250 [154.25]	125.3300 [241.10]
Valine	0.019376	1.3453	0.60479	529.5950 [455.44]	323.2700 [317.20]

Differential metabolites were selected according to $VIP > 1$, $FC > 1.3$, and $p < 0.05$. Values are expressed as medians [IQR]. P-values were calculated from a t-test for continuous variables; VIP, variable influence on projection; CMT, Charcot-Marie-Tooth disease.

Continuing the analysis, differential metabolites were also examined between the overall CMT patient group and the control group. Two plasma metabolites were identified with significantly different levels in patients compared to healthy individuals (Figure 2.6 (a and b)). CMT patients showed elevated plasma acetylcarnitine levels and reduced glycine levels in comparison to the control group (Mann–Whitney U test: $U = 1773.000$, $p = 0.04$ for acetylcarnitine; $U = 1018.000$, $p = 0.15$ for glycine) (Figure 2.6 (c); Table 2.5).

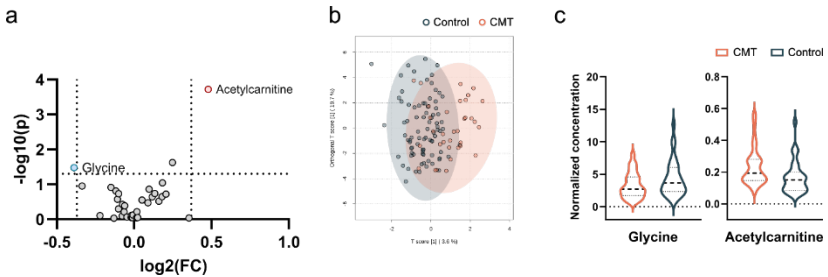


Figure 2.6 Visualisation of differential metabolite profiles in all CMT cases compared to healthy controls using a V-plot

Significance thresholds are indicated with dashed lines ($FC > 1.3$, $p < 0.05$).

b. OPLS-DA score plot of CMT versus control. c. Violin plot of glycine and acetylcarnitine as the significant metabolites identified in the V-plot ($p < 0.05$).

Table 2.5

Differential plasma metabolites between CMT patients and healthy controls

Metabolite	p-value	VIP	FC	Control group (median [IQR])	CMT (median [IQR])
Acetylcarnitine	2.7234E-4	2.232	1.3883	10.8350 [9.86]	13.4850 [7.49]
Glycine	0.03318	1.5599	0.76581	299.9250 [154.25]	194.5500 [224.53]

Differential metabolites were selected according to $VIP > 1$, $FC > 1.3$, and $p < 0.05$. Values are expressed as medians [IQR]. P-values were calculated from a t-test for continuous variables; VIP, variable influence on projection; CMT, Charcot-Marie-Tooth disease.

2.5.1 Predictive abilities of CMT-related biomarkers

This study evaluated the potential of plasma metabolite levels and their ratios to classify CMT patients using machine learning algorithms. Separate analyses were conducted to assess the ability to distinguish CMT1A and CMTX1 patient subgroups. For each case, classification models were developed, and group discrimination was evaluated using receiver operating characteristic (ROC) curves. The quality of the models was assessed by calculating the area under the curve (AUC). Across all models, predictive performance was limited, with AUC values below 0.74 (Figure 2.7). A more detailed analysis was conducted for the CMT1A group (Figure 2.8 (a)), and a predictive model was constructed using a multivariate regression approach with three features. ROC analysis of this model yielded an AUC of 0.73 (Figure 2.8 (b)), indicating limited ability to distinguish CMT1A samples from other samples (Figure 2.8 (c)).

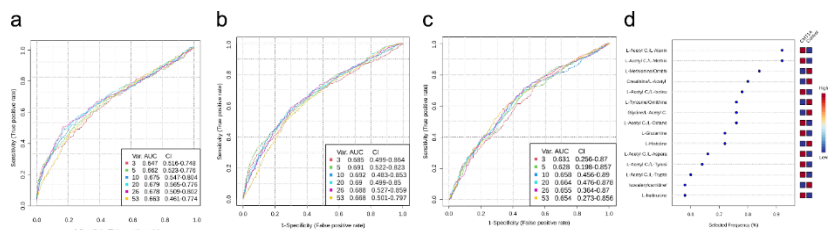


Figure 2.7 Comparison of classification models for CMT (a), CMT1A (b), and CMTX1 (c), along with relative importance of metabolites in CMT1A model (d)

Comparison of classification models for CMT with different numbers of variables (right bottom box) using linear support vector machine algorithm for classification and RandomForest as ranking method for a. total CMT, b. CMT1A, and c. CMTX1. d. Feature importance for classification of CMT1A.

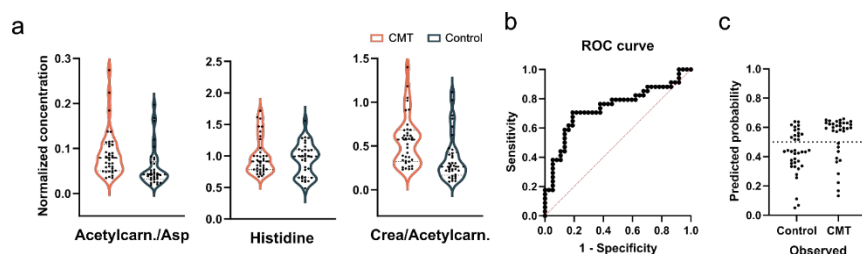


Figure 2.8 CMT1A prognostic model

Violin plots of one metabolite and two ratios were used for the CMT1A predictive model. Concentrations were normalised to the average of each sample. ANOVA with Bonferroni correction shows no significant differences. b. ROC curves of a predictive model based on multiple linear regression and c. classifications of samples using the constructed model.

2.5.2 Metabolic profiles in CMT of different severity

All CMT patients (n = 66) who underwent disease severity assessment using the CMTNSv2 scale were classified into three severity categories: mild (CMTNSv2 score 0–10; n = 34), moderate (score 11–20; n = 27), and severe (score \geq 21; n = 5). Principal component analysis (PCA) and orthogonal partial least squares discriminant analysis (OPLS-DA) identified two differential metabolites between the moderate and severe CMT groups ($p < 0.05$; VIP > 1;

FC > 1) (Table 2.6). When comparing mild and severe disease groups, one differential metabolite was identified (Table 2.7).

Table 2.6

Differential plasma metabolites between moderate and severe CMT patients

Metabolite	p-value	VIP	FC	Moderate CMT (median [IQR])	Severe CMT (median [IQR])
Tyrosine	0.023081	1.8717	0.74866	80.7300 [64.82]	77.1100 [88.74]
Acetylcarnitine	0.033947	2.09858	0.67648	12.6300 [6.73]	16.1300 [16.80]

Differential metabolites were selected according to VIP > 1, FC > 1.3, and p < 0.05. Values are expressed as medians [IQR]. P-values were calculated from a t-test for continuous variables; VIP, variable influence on projection; CMT, Charcot-Marie-Tooth disease.

Table 2.7

Differential plasma metabolites between mild and severe CMT patients

Metabolite	p-value	VIP	FC	Mild CMT (median [IQR])	Severe CMT (median [IQR])
Proline	0.024678	1.3111	0.73151	291.2650 [196.39]	311.5200 [142.87]

Differential metabolites were selected according to VIP > 1, FC > 1.3, and p < 0.05. Values are expressed as medians [IQR]. P-values were calculated from a t-test for continuous variables; VIP, variable influence on projection; CMT, Charcot-Marie-Tooth disease.

However, when comparing patients across different CMT severity levels with the control group, no significant differences were found in the levels of tyrosine, acetylcarnitine, or proline (two-way ANOVA with Tukey's multiple comparison test). Furthermore, correlation analysis did not identify any metabolite with a correlation coefficient greater than 0.5. This indicates a weak association between the analysed metabolites and disease severity (Figure 2.9).

Discussion

This study evaluated the clinical manifestations of CMT and the dynamic changes in plasma NfL concentrations, including the relationship between NfL fluctuations and disease progression in both adult and paediatric patient cohorts. Additionally, plasma metabolites were quantified across different CMT subgroups, and their association with the severity of clinical manifestations was analysed.

The CMT patient cohort in this study consisted of 101 individuals, with a definitive genetic cause of the disease identified in 80 cases. It is known that a precise genetic diagnosis can be established in approximately 60–80 % of patients with CMT. Reviewing current genetic testing algorithms reveals that up to 90 % of genetically confirmed CMT cases are attributable to pathogenic variants in four major genes: *PMP22*, *MPZ*, *GJB1*, and *MFN2*. Expanding the analysis to include four additional commonly implicated genes – *GDAP1*, *HINT1*, *SH3TC2*, and *SORD* – via multigene panels can further increase the diagnostic yield. The diagnostic yield from CMT multigene panel testing varies between 18 % and 31 %, depending on the specific characteristics of the tested population and the number and type of genes included in the panel. For patients in whom prior genetic testing has not revealed a pathogenic variant, the next diagnostic step may involve exome sequencing (ES), and in some cases, whole genome sequencing (WGS). ES can help confirm a genetic diagnosis in approximately 19–45 % of such cases, especially when accompanied by detailed phenotypic information, which facilitates targeted interpretation of sequencing data. In this study, using the above - mentioned strategies, the genetic cause of disease remained undetermined in 21 % of patients, which is consistent with findings reported in other studies (Bird, 2025; Felice et al., 2021; Fridman et al., 2015; Padilha et al., 2020; Pipis et al., 2019; Ramchandren, 2017; Rudnik-Schöneborn et al., 2016; Saporta et al., 2011).

In this study cohort, ES identified two unique, previously unreported variants in the *AARS1* gene – c.1823C>A p.(Thr608Lys) and c.1815C>G p.(His605Gln) – in two patients. Pathogenic variants in *AARS1* are associated with CMT2N, a rare axonal subtype of Charcot-Marie-Tooth disease. To date, both the genetic and phenotypic spectrum of CMT2N remains incompletely understood, with most available data derived from isolated case reports or small patient cohorts. A review of the literature has documented 37 distinct *AARS1* variants reported in 90 patients across 32 families. Both in the patients identified in this study and those previously described in the literature, the common clinical manifestations include distal muscle weakness in both lower and upper extremities, foot drop, gait difficulties, lower limb pain, numbness and hypoesthesia in the lower legs, feet, and toes, as well as *pes cavus* deformity. Electrophysiological evaluation in these patients typically reveals an axonal or intermediate form of CMT, characterised by motor nerve conduction velocities ranging from 25 to 45 m/s. (Berciano et al., 2017). In summary, pathogenic variants in the *AARS1* gene cause a slowly progressive, sensorimotor axonal or intermediate form of polyneuropathy, which is often characterised by asymmetric symptom presentation and variable age of onset, without apparent involvement of other organ systems. These findings expand the current understanding of the genotypic and phenotypic heterogeneity of CMT and provide a significant contribution to the diagnosis and analysis of *AARS1*-related CMT.

In this study, the CMTNSv2 was used for clinical patient assessment, incorporating both clinical and electrophysiological parameters. Electrophysiological data were obtained through standardised nerve conduction studies (NCS). Based on the conduction velocity in the upper limbs – which reflects myelin function – CMT neuropathy can be classified into different forms. A normal or only mildly reduced conduction velocity is characteristic of the axonal form (CMT2), typically associated with reduced compound muscle

action potential (CMAP) amplitudes, indicating predominant axonal damage with relatively preserved myelin function. In intermediate forms, conduction velocities are moderately reduced (25–45 m/s), whereas in demyelinating forms (CMT1), conduction velocities are significantly reduced (< 35 m/s), reflecting primary myelin dysfunction. Although this study did not separately analyse the correlation between electrophysiological CMT subtypes and potential biomarkers, it is important to note that the majority of patients ($n = 78$) exhibited a demyelinating form (CMT1). Sixteen patients had prolonged latencies and reduced amplitudes with relatively preserved conduction velocity, consistent with an axonal form (CMT2). Six patients showed both demyelinating and axonal features, indicative of an intermediate form. In one patient, no neuropathic abnormalities were detected on nerve conduction studies; however, this individual was included in the study based on genetic confirmation of CMT1A. Asymptomatic presentations of CMT1A without detectable neurophysiological changes have previously been described in the literature (Jariwal et al., 2018; Vaeth et al., 2021).

To assess the progression of CMT over time, this study included a follow-up clinical evaluation of 73 patients after a 3-year interval. Disease progression was evaluated using the CMTNSv2 scale as the primary outcome measure. Although the mean score showed an increase over time, indicating disease progression, the changes were relatively small (median change = 1.0, IQR = 3.0). Similar longitudinal changes in CMTNSv2 scores over time have also been reported in previous studies involving CMT patients (Fridman et al., 2020; Rossor et al., 2022). These findings confirm the well-established understanding that CMT is a clinically slowly progressive polyneuropathy with a broad spectrum of clinical manifestations and disease severity, which can vary even among individuals within the same genetic subgroup (Bird, 2025). However, it should be noted that this scale does not fully reflect all possible

symptoms or clinical and neurophysiological findings of hereditary neuropathy. A low score does not always accurately represent the patient's functional impairments or limitations in daily activities. Neurophysiologically, the scale may also inadequately capture the severity of polyneuropathy, as it only includes functional parameters from upper limb nerves, which may still be unaffected in the early stages of the disease. This limitation creates a risk of falsely negative neurophysiological assessments. To obtain a more accurate evaluation of disease severity, it may be useful to consider including functional parameters of lower limb nerves in the assessment. However, it must be taken into account that these nerves often already exhibit significant changes at an early stage, which may reduce their usefulness for dynamic follow-up in repeated assessments. Overall, these factors highlight the need to develop more appropriate and sensitive tools for evaluating the clinical status of patients.

Neurofilament light chain concentration in plasma as a biomarker of CMT progression

In this study, plasma NfL concentrations were longitudinally assessed in CMT patients and control group individuals over a three-year follow-up period. The association between changes in NfL levels and clinical disease progression was analysed to evaluate the potential of NfL as a biomarker for CMT progression.

In this study, the absolute concentrations of plasma NfL were generally lower than those reported in earlier publications, indicating potential methodological or cohort-related differences (Khalil et al., 2020; Sandelius et al., 2018). In addition to the previously mentioned influencing factors, these differences may be due to the fact that NfL levels were measured in different laboratories using various methods. Currently, there is no standardised method for determining NfL concentration, nor are there globally defined reference intervals. This highlights the need to develop a standardised test and harmonise

the determination of threshold values across laboratories to enable effective use of NfL in clinical practice. It is important to emphasise that in this study, the repeated measurement of plasma NfL concentration for both patients and control group participants was performed under identical conditions – in the same laboratory and using the same method as in the initial assessment.

Several studies to date have already demonstrated elevated plasma NfL concentrations in CMT patients compared to healthy individuals (Millere et al., 2021; Sandelius et al., 2018). In this study, to ensure comparable results, both CMT patients and control group participants were evaluated under similar conditions using the same NfL detection methods. As reported in previous studies, plasma NfL levels were elevated in CMT patients compared to the control group. When analysing NfL concentrations across specific genetic subtypes of CMT, significant differences were observed only in certain groups: CMT1A, CMTX1, CMT2A, and inherited neuropathies associated with *HINT1* gene variants. Although we detected a difference in NfL levels between CMT patients and controls, the potential influence of other confounding factors cannot be ruled out. Further studies are necessary to gain a deeper understanding of the mechanisms underlying NfL elevation in CMT.

Due to the clinical heterogeneity and slow progression of CMT disease, it remains challenging to develop sensitive clinical outcome measures and biomarkers. Current data suggest that NfL has significant potential as a biomarker in peripheral nervous system disorders. Recently, an association between CMT disease severity (assessed using disease-specific clinical scales) and plasma NfL concentration has been described (Millere et al., 2021; Rossor et al., 2022; Sandelius et al., 2018). In contrast to previously published data showing a moderate to strong correlation between CMTNSv2 and NfL levels, no significant correlation between these parameters was observed in this study

cohort. This suggests that plasma NfL concentration may not be a reliable biomarker for the clinical severity of CMT.

One of the main objectives of this study was to evaluate whether NfL levels could serve as a biomarker for CMT progression. Recently published study by Rossor et al. showed longitudinal data of 27 CMT patients (Rossor et al., 2022). Plasma NfL concentration was repeatedly measured after 6 years; however, no significant changes in NfL levels were observed. Sandelius et al. (Sandelius et al., 2018) published longitudinal data on 9 CMT patients and 13 control group participants. Study participants were re-evaluated after one year, and no significant changes in plasma NfL levels were observed. In our study, follow-up clinical assessment and NfL level determination were performed in a comparatively larger cohort – 73 CMT patients and 28 healthy controls. It is worth noting that the dynamic evaluation was conducted only after 3 years due to restrictions related to the COVID-19 pandemic. However, considering that CMT is a slowly progressive disease, a longer interval between assessments may improve the likelihood of detecting biomarker level changes. As a result, we observed that the NfL concentration had significantly increased at the 3-year follow-up compared to baseline. These changes were noted in both the CMT and control groups. Interestingly, NfL levels decreased over time in 22 patients. Among them were individuals with CMT1A, CMT2A, CMTX1, CMT2F, HMN5C, and SMALED2A genotypes, three patients without an identified monogenic cause, and seven participants from the control group. The reasons for these decreases remain unclear; however, a decline in NfL levels over time in CMTX1 patients has been reported before (Rossor et al., 2022). Although the overall trend indicated an increase in NfL concentration in both the CMT and control groups, it is important to highlight the differences observed among individual participants and across various genetic subtypes of CMT.

This suggests that dynamic changes in NfL levels are nonspecific – they vary between patients and controls, across different ages, and between disease types.

In this study, patients underwent a follow-up clinical assessment three years after the initial evaluation, during which the CMTNSv2 score was reassessed to reflect disease progression. To investigate whether NfL could serve as a reliable biomarker of CMT progression, a correlation analysis was conducted between the changes in plasma NfL levels and changes in CMTNSv2 scores over the same period. Similar approach has been reported in another recently published study (Rossor et al., 2022). Unlike expectations, no statistically significant correlation was found (Spearman's $r = 0.228$, $p = 0.052$). These findings suggest that plasma NfL levels may have limited value in monitoring disease progression in CMT patients.

In all previously published CMT patient cohorts where NfL concentration was analysed, the average age of participants exceeded 18 years. Therefore, in this study, an additional analysis was conducted for paediatric patients to explore whether NfL measurement – reflecting the rate of axonal degeneration – might be more informative in younger individuals at early disease stages. A total of 19 CMT patients under the age of 18 were included in this analysis, with repeated NfL measurements available for 11 of them after a 3-year follow-up. The results showed a decrease in NfL levels over time in the paediatric group compared to baseline. Although the CMTPedS is typically used to assess disease severity in children, the CMTNSv2 scale was applied uniformly across all patients in this study, including paediatric cases. Since CMTNSv2 captures similar clinical features, it was considered appropriate for evaluating functional impairment in children within this research context (Burns et al., 2013). When comparing changes in NfL levels over time with disease progression in this cohort, no significant correlation was observed between these two parameters. However, it should be noted that the number of analysed paediatric patients was relatively

small, and an age-matched control group was not included in the analysis. Despite these limitations, the findings highlight the need for additional data to determine whether plasma NfL levels can reliably reflect disease progression in the paediatric CMT population.

The data from this study contribute to the existing knowledge regarding plasma NfL levels as a potential biomarker in CMT disease. The study evaluated longitudinal changes in NfL levels in both adult and paediatric patients and analysed the ability of NfL to reflect disease progression. Although overall NfL concentrations were higher in CMT patients compared to healthy individuals, the dynamic changes in NfL levels varied across different CMT genetic subtypes and age groups. Moreover, the study demonstrated no association between changes in plasma NfL levels and clinical disease progression. Therefore, NfL concentration does not reflect disease severity or progression rate and cannot be reliably used as a biomarker for monitoring disease progression in CMT studies.

Plasma metabolites as biomarkers of CMT

A large cohort of CMT patients with well-characterised phenotypes and a healthy control group was included in this study to analyse the plasma metabolome and identify plasma metabolites that could serve as potential biomarkers for CMT. Furthermore, this study identified differential plasma metabolites across various CMT subtypes and evaluated their correlation with the clinical severity of the disease.

This study applied a targeted metabolomics approach to analyse blood samples from CMT patients and control group participants, measuring a total of 33 metabolites. The selection of these specific metabolites was based on both technical and practical considerations. In total, 53 metabolites were initially targeted, of which 33 were successfully detected in plasma samples (Annex 4). These included amino acids, amino acid derivatives, acylcarnitines, and biogenic amines. These metabolites were selected due to the availability of standard

compounds and isotopically labelled internal standards, which are essential for accurate quantitative analysis. Moreover, their relatively high concentrations in blood make them suitable for reliable and reproducible quantification – a critical requirement for identifying robust biomarkers. Importantly, most of these metabolites are already routinely measured by mass spectrometry in newborn screening programmes (Lehotay et al., 2011), and standardised, certified methods are available for their analysis. Therefore, alterations in the plasma metabolome of CMT patients, identified through these established methods, could serve as a practically applicable and easily implementable diagnostic tool in clinical practice.

The analysis of the plasma metabolome may be affected by multiple factors, including aspects of sample collection and processing, patient-specific biological characteristics, and the analytical techniques used in metabolomic profiling (Lehmann, 2021; Thachil et al., 2024). For example, a recently published study analysed 1183 plasma metabolites in a broadly phenotyped cohort of 1368 individuals (Chen et al., 2022). The study identified 610 metabolites primarily associated with diet, 85 metabolites linked to the gut microbiome, and 38 metabolites related to genetic factors. However, our study did not examine associations with other individual participant characteristics, which are nonetheless essential to consider when identifying new potential disease biomarkers.

Proper sample collection, processing, and other pre-analytical steps are particularly important, since metabolites may undergo changes before they are measured with a given analytical platform (Lin et al., 2024; Sens et al., 2023). Therefore, it is essential to develop and implement standardised procedures for sample collection, processing, and data acquisition. Another major limitation in metabolomics is the challenge of accurately identifying and quantifying metabolites, which is addressed by applying specific statistical software and

bioinformatics tools. Standardisation of all these steps is crucial to ensure reproducibility of results and the reliable identification of potential biomarkers. Moreover, successful implementation of metabolite biomarkers in clinical practice requires their validation in larger populations (Sarmad et al., 2023).

In this study, out of the 33 plasma metabolites analysed, two metabolites – acetylcarnitine and glycine – were identified as differential metabolites between CMT patients and the control group. Acetylcarnitine levels were elevated in the CMT group compared to controls, while glycine levels were reduced in CMT patients in relation to healthy individuals.

The study data demonstrated elevated acetylcarnitine levels in the CMT patient group compared to the control group. Similar findings were observed in specific genetic subtypes, with increased acetylcarnitine concentrations particularly evident in the CMT1A subgroup. Acetylcarnitine is a biologically active compound formed from carnitine and acetyl-coenzyme A via the action of carnitine acetyltransferase. Its primary role is to regulate cellular energy homeostasis, particularly under conditions of enhanced carbohydrate oxidation, such as during physical exertion or hypoxia. In states of intensified mitochondrial activity, excessive production of acetyl-CoA can exceed the capacity of the Krebs cycle. Carnitine reacts with acetyl-CoA to form acetylcarnitine, thereby liberating free CoA, which is essential for the pyruvate dehydrogenase complex and other key metabolic processes. This reaction facilitates continued carbohydrate oxidation and prevents the accumulation of intermediates that could disrupt cellular energetics. Thus, acetylcarnitine acts as a metabolic buffer, supporting mitochondrial flexibility by sustaining energy production and modulating the balance between fatty acid and carbohydrate utilisation in ATP synthesis.

Its elevation may represent an adaptive mechanism to maintain free coenzyme A availability and ensure ongoing Krebs cycle and pyruvate

dehydrogenase activity (Adams et al., 2009; Evans & Fornasini, 2003; Noland et al., 2009; Reuter & Evans, 2012).

Altered acetylcarnitine concentrations have been observed in several genetic disorders; therefore, deviations from normal acetylcarnitine levels may serve as diagnostic indicators for inherited metabolic diseases. (Clayton et al., 2001; Hori et al., 2010). Furthermore, altered acetylcarnitine levels have also been identified in various chronic metabolic, oncological, and cardiovascular diseases (Adams et al., 2009; Ciborowski et al., 2015; Cristofano et al., 2016; Mai et al., 2013; Steiner et al., 2018; Takaya et al., 2019; Ueland et al., 2013; Zordoky et al., 2015). To date, no published data exist regarding changes in acetylcarnitine levels in CMT. However, it is known that elevated acetylcarnitine levels in patients with diabetes have been associated with an increased risk of developing diabetic polyneuropathy (An et al., 2022). Studies on diabetic neuropathy suggest that insulin resistance leads to mitochondrial dysfunction in Schwann cells, resulting in nerve demyelination and axonal loss. In addition, this condition promotes a metabolic shift from fatty acid synthesis to fatty acid oxidation, enhancing the formation and accumulation of acylcarnitines, including acetylcarnitine. This secondary accumulation may further exacerbate nerve damage (Hackett et al., 2020; Viader et al., 2013). It remains unclear whether the mechanism leading to elevated acetylcarnitine levels is pathognomonic solely for diabetic neuropathy or represents a more general, nonspecific response also present in other types of neuropathies, including genetic forms. Although the pathogenic role of acetylcarnitine and its association with the development of polyneuropathy in diabetes is well established, its involvement in hereditary neuropathies remains poorly understood. Notably, one study on CMT with episodic rhabdomyolysis associated with a defect in the mitochondrial trifunctional protein β -subunit described increased levels of long-chain acylcarnitines in plasma, but did not observe elevated acetylcarnitine

levels (Guan et al., 2021). However, in order to evaluate the significance of altered acetylcarnitine levels in CMT, additional data from cohorts of patients with hereditary neuropathies are needed. Moreover, standardised metabolomic methodologies and established reference ranges for acetylcarnitine concentrations are essential for meaningful interpretation.

In this study, metabolomic analysis revealed a reduced glycine concentration in CMT patients compared to healthy participants. When examining specific genetic subtypes of CMT, a decreased glycine level was also observed in the CMTX1 patient group. Additionally, CMTX1 patients exhibited lower levels of L-valine. It is known that low systemic glycine levels are considered an indicator of peripheral nervous system dysfunction and are associated with the development of peripheral neuropathy (Handzlik et al., 2023). Moreover, a study in mice has demonstrated that dietary restriction of serine and glycine over a 10-month period promotes the development of peripheral sensory deficits (Gantner et al., 2019). Metabolomics studies in diabetic patients have reported that the biosynthesis of valine, leucine, and isoleucine is one of the key metabolic pathways involved in the development of diabetic polyneuropathy (Shao et al., 2022). Although the aforementioned studies suggest a role for glycine and valine in the development of peripheral neuropathy, the precise mechanisms by which these metabolites are involved remain unclear. In the present study, a reduced concentration of L-valine was observed only in one genetic subgroup - CMTX1. Therefore, it remains uncertain whether these metabolites could serve as specific biomarkers for CMT in the future.

In this study, machine learning algorithms were applied to assess the potential of plasma metabolite levels and their ratios for classifying CMT patients. Predictive models were developed using varying numbers of variables to differentiate CMT subgroups. ROC analysis and AUC calculations were performed for each model; however, predictive performance across all models

was limited, as AUC values remained below 0.74. Previous studies have reported 12 plasma metabolites associated with CMT1A, of which four (glutamyl-serine, sphingosine-1-phosphate, tryptophan, and leucine) showed strong biomarker potential with AUC values exceeding 0.889 (Soldevilla et al., 2017). In contrast, only one of these metabolites (leucine) was included in the present analysis of 33 metabolites, and it did not show significant discriminative power between patients and controls. Although this study identified a distinct metabolite (acetylcarnitine) in the CMT1A group, the model's ability to differentiate this subgroup from others was weak ($AUC < 0.73$).

In this study, the metabolic profile was additionally analysed across different clinical severity levels of Charcot-Marie-Tooth (CMT) disease with the aim of identifying potential biomarkers for monitoring disease progression. Patients were categorised into three groups according to disease severity: mild, moderate, and severe. Among the identified metabolites, tyrosine, acetylcarnitine, and proline initially showed statistically significant differences when comparing the mild and severe groups as well as the moderate and severe groups. However, in subsequent analyses comparing these metabolite levels across the severity groups and the control group, no significant differences were observed. In comparison, a study by Soldevilla et al. (Soldevilla et al., 2017) involving 42 CMT1A patients and 15 healthy controls identified five metabolites (urobilinogen, glutamyl-serine, sphingosine-1-phosphate, palmitamide, and leucine) that showed a strong and statistically significant correlation with disease severity (Spearman's coefficient > 0.629). Based on those findings, this study also conducted a correlation analysis between plasma metabolite levels and clinical severity using the CMTNSv2 scale. The results, however, revealed that none of the analysed metabolites had a correlation coefficient greater than 0.5, indicating a weak association. This included leucine, which was the only metabolite examined in both studies, but in the present analysis, it did not show

a statistically significant correlation with disease severity. Despite a larger cohort and broader representation of genetic CMT subtypes, the results of this study do not support a correlation between metabolite levels and disease severity, including for leucine.

To date, there have been no studies or published data on the metabolome in paediatric CMT cohorts. Although a separate results section for the paediatric group was not included in this study due to the small number of patients, it is important to highlight the observed trends in metabolomic analysis of children with CMT. The analysed cohort consisted of 12 CMT patients (half of whom had a confirmed CMT1A diagnosis) and 5 individuals in the control group. When comparing the overall paediatric CMT group to controls, significantly elevated levels of butyrylcarnitine and valine, as well as decreased levels of cystine, were observed in the patient group. In a separate analysis of paediatric CMT1A patients, additional differences were identified: significantly increased levels of carnitine and acetylcarnitine and a reduced level of taurine were observed compared to healthy controls. At present, the biomarker potential of these metabolites in the paediatric cohort remains unclear due to the limited sample size, the small control group, and the lack of longitudinal data or comparable paediatric CMT metabolomic profiles in other studies.

This study provides data on plasma metabolite levels in CMT patients. It was found that patients with CMT had significantly elevated levels of acetylcarnitine and reduced levels of glycine compared to the control group. Additionally, in the CMTX1 subgroup, a decreased level of valine was also observed in comparison to controls. Despite these statistically significant differences, the constructed predictive models did not demonstrate strong predictive ability for any of the CMT groups. Furthermore, no association was found between the identified metabolites and disease severity. Therefore, these

metabolites may not be specific biomarkers for CMT; however, longitudinal studies are needed to assess their potential as biomarkers for disease progression.

Study limitations

This study had several limiting factors that may have influenced the generalisability of some of the results. One such factor was the relatively small number of patients included in certain genetic subgroups, which did not always allow a full assessment of differences between groups with adequate statistical significance. Increasing the number of patients in these groups could yield more statistically significant results. It should be noted that in the analysis of NfL levels between the patient and control groups, the calculated statistical power exceeded 80 %; however, in the metabolomics analysis it did not surpass the 80 % threshold. Future studies should increase the number of individuals in the control group to obtain clinically meaningful and statistically robust results.

Conclusions

- 1 Repeated clinical and neurophysiological assessment after three years in CMT patients showed mild increase in the disease severity, indicating slow disease progression.
- 2 Plasma NfL levels are elevated in CMT patients compared to the control group; however, they are not associated with disease severity.
- 3 Changes in NfL concentration over three years do not correlate with clinical progression of CMT.
- 4 CMT patients have significantly elevated acetylcarnitine and reduced glycine levels, and reduced valine levels in the CMTX1 group compared to controls.
- 5 Classification of CMT patients based on plasma metabolite concentrations shows limited predictive value, and metabolite concentration changes do not correlate with disease severity.

Proposals

- 1 For monitoring CMT patients, structured and repeated clinical assessment methods – such as the CMTNSv2 scale – are recommended, as they allow for objective long-term evaluation of disease progression.
- 2 Plasma NfL concentration may be used as a supportive marker in differential diagnosis or as a secondary marker in research; however, its use for evaluating disease progression is not recommended.
- 3 Targeted metabolomic analysis, despite identifying significant differences, is not yet applicable for individual disease course prediction. Broader validation of metabolite profiles across different CMT subtypes is required to determine their potential for use in personalised medicine.
- 4 Future studies should be designed as longitudinal studies with more frequent follow-up time points and larger patient cohorts, allowing for the evaluation of biomarker sensitivity, correlation with clinical changes, and their possible integration with imaging, genetic, or other biochemical markers.

List of publications

Publications:

1. Setlere S, Jurcenko M, Gailite L, Rots D, Kenina V. Alanyl-tRNA Synthetase 1 Gene Variants in Hereditary Neuropathy: Genotype and Phenotype Overview. *Neurol Genet.* 2022 Sep 5;8(5):e200019. doi: 10.1212/NXG.0000000000200019. PMID: 36092982; PMCID: PMC9450682.
2. Setlere S, Grosmane A, Kurjane N, Gailite L, Rots D, Blennow K, Zetterberg H, Kenina V. Plasma neurofilament light chain level is not a biomarker of Charcot-Marie-Tooth disease progression: Results of 3-year follow-up study. *Eur J Neurol.* 2023 Aug;30(8):2453-2460. doi: 10.1111/ene.15858. Epub 2023 Jun 5. PMID: 37165526.
3. Setlere S, Schiemer T, Vaska A, Gailite L, Rots D, Kenina V, Klavins K. Metabolomics insights into Charcot-Marie-Tooth disease: toward biomarker discovery. *Front Neurol.* 2025 May 19;16:1543547. doi: 10.3389/fneur.2025.1543547. PMID: 40458460; PMCID: PMC12127190.

Reports and theses at international congresses and conferences:

1. Setlere, S., Millere, E., Kupats, E., Rots, D., Mičule, I., Gailite, L., Kenina, V. 2021. Genotype-phenotype associations in Charcot-Marie-Tooth disease. *79th Scientific Conference of the University of Latvia.* Riga, Latvia.
2. Setlere, S., Kalniņa, M., L., Grosmane, A., Kurjane, N., Gailite, L., Rots, D., Blennow, K., Zetterberg, H., Kenina, V. 2023. Paediatric Charcot-Marie-Tooth disease: longitudinal evaluation of potential disease progression biomarkers. RSU international conference on medical and health care sciences *Knowledge for use in practice*, Rīga, Latvia.
3. Setlere, S., Millere, E., Jurcenko, M., Micule, I., Gailite, L., Kazaine, I., Dīriks, M., Rots, D., Kenina, V. 2022. Charcot-Marie-Tooth disease in paediatric patients. *16th Conference of Baltic Child Neurology Association*, Parnu, Estonia.
4. Setlere, S., Schiemer, T., Vaska, A., Gailite, L., Rots, D., Klavins, K., Kenina, V. 2024. Searching for metabolic markers of Charcot-Marie-Tooth disease. *17th Conference of Baltic Child Neurology Association*, Jūrmala, Latvija.
5. Setlere, S., Schiemer, T., Vaska, A., Gailite, L., Rots, D., Klavins, K., Kenina, V. 2024. Biomarkers in Hereditary Neuropathies: Current Insights. *4th Baltic School of neuromyology*, Tallinn, Estonia. 23–24.08.2024

References

1. Adams, S. H., Hoppel, C. L., Lok, K. H., Zhao, L., Wong, S. W., Minkler, P. E., Hwang, D. H., Newman, J. W., & Garvey, W. T. (2009). Plasma acylcarnitine profiles suggest incomplete long-chain fatty acid beta-oxidation and altered tricarboxylic acid cycle activity in type 2 diabetic African-American women. *J Nutr*, 139(6), 1073–1081. <https://doi.org/10.3945/jn.108.103754>
2. Akbar, M., Bhandari, U., Habib, A., & Ahmad, R. (2017). Potential Association of Triglyceride Glucose Index with Cardiac Autonomic Neuropathy in Type 2 Diabetes Mellitus Patients. *J Korean Med Sci*, 32(7), 1131–1138. <https://doi.org/10.3346/jkms.2017.32.7.1131>
3. An, Z., Zheng, D., Wei, D., Jiang, D., Xing, X., & Liu, C. (2022). Correlation between Acylcarnitine and Peripheral Neuropathy in Type 2 Diabetes Mellitus. *J Diabetes Res*, 2022, 8115173. <https://doi.org/10.1155/2022/8115173>
4. Berciano, J., García, A., Gallardo, E., Peeters, K., Pelayo-Negro, A. L., Álvarez-Paradelo, S., Gazulla, J., Martínez-Tames, M., Infante, J., & Jordanova, A. (2017). Intermediate Charcot-Marie-Tooth disease: an electrophysiological reappraisal and systematic review. *J Neurol*, 264(8), 1655–1677. <https://doi.org/10.1007/s00415-017-8474-3>
5. Bird, T. D. (2025). *Charcot-Marie-Tooth Hereditary Neuropathy Overview*. In M. P. Adam, J. Feldman, G. M. Mirzaa, R. A. Pagon, S. E. Wallace, & A. Amemiya (Eds.), *GeneReviews*(®). University of Washington, Seattle. Copyright © 1993–2025, University of Washington, Seattle. GeneReviews is a registered trademark of the University of Washington, Seattle. All rights reserved.
6. Burns, J., Menezes, M., Finkel, R. S., Estilow, T., Moroni, I., Pagliano, E., Laurá, M., Muntoni, F., Herrmann, D. N., Eichinger, K., Shy, R., Pareyson, D., Reilly, M. M., & Shy, M. E. (2013). Transitioning outcome measures: relationship between the CMTPedS and CMTNSv2 in children, adolescents, and young adults with Charcot-Marie-Tooth disease. *J Peripher Nerv Syst*, 18(2), 177–180. <https://doi.org/10.1111/jns5.12024>
7. Chen, L., Zhernakova, D. V., Kurilshikov, A., Andreu-Sánchez, S., Wang, D., Augustijn, H. E., Vich Vila, A., Weersma, R. K., Medema, M. H., Netea, M. G., Kuipers, F., Wijmenga, C., Zhernakova, A., & Fu, J. (2022). Influence of the microbiome, diet and genetics on inter-individual variation in the human plasma metabolome. *Nat Med*, 28(11), 2333–2343. <https://doi.org/10.1038/s41591-022-02014-8>
8. Ciborowski, M., Adamska, E., Rusak, M., Godzien, J., Wilk, J., Citko, A., Bauer, W., Gorska, M., & Kretowski, A. (2015). CE-MS-based serum fingerprinting to track evolution of type 2 diabetes mellitus. *Electrophoresis*, 36(18), 2286–2293. <https://doi.org/10.1002/elps.201500021>

9. Clayton, P. T., Eaton, S., Aynsley-Green, A., Edginton, M., Hussain, K., Krywawych, S., Datta, V., Malingre, H. E., Berger, R., & van den Berg, I. E. (2001). Hyperinsulinism in short-chain L-3-hydroxyacyl-CoA dehydrogenase deficiency reveals the importance of beta-oxidation in insulin secretion. *J Clin Invest*, 108(3), 457–465. <https://doi.org/10.1172/jci11294>
10. Cornett, K. M. D., Wojciechowski, E., Sman, A. D., Walker, T., Menezes, M. P., Bray, P., Halaki, M., & Burns, J. (2019). Magnetic resonance imaging of the anterior compartment of the lower leg is a biomarker for weakness, disability, and impaired gait in childhood Charcot-Marie-Tooth disease. *Muscle Nerve*, 59(2), 213–217. <https://doi.org/10.1002/mus.26352>
11. Cristofano, A., Sapere, N., La Marca, G., Angiolillo, A., Vitale, M., Corbi, G., Scapagnini, G., Intrieri, M., Russo, C., Corso, G., & Di Costanzo, A. (2016). Serum Levels of Acyl-Carnitines along the Continuum from Normal to Alzheimer's Dementia. *PLoS One*, 11(5), e0155694. <https://doi.org/10.1371/journal.pone.0155694>
12. Dortch, R. D., Dethrage, L. M., Gore, J. C., Smith, S. A., & Li, J. (2014). Proximal nerve magnetization transfer MRI relates to disability in Charcot-Marie-Tooth diseases. *Neurology*, 83(17), 1545–1553. <https://doi.org/10.1212/wnl.0000000000000919>
13. Ebenezer, G. J., Hauer, P., Gibbons, C., McArthur, J. C., & Polydefkis, M. (2007). Assessment of epidermal nerve fibers: a new diagnostic and predictive tool for peripheral neuropathies. *J Neuropathol Exp Neurol*, 66(12), 1059–1073. <https://doi.org/10.1097/nen.0b013e31815c8989>
14. Eggermann, K., Gess, B., Häusler, M., Weis, J., Hahn, A., & Kurth, I. (2018). Hereditary Neuropathies. *Dtsch Arztebl Int*, 115(6), 91–97. <https://doi.org/10.3238/arztebl.2018.0091>
15. Evans, A. M., & Fornasini, G. (2003). Pharmacokinetics of L-carnitine. *Clin Pharmacokinet*, 42(11), 941–967. <https://doi.org/10.2165/00003088-200342110-00002>
16. Felice, K. J., Whitaker, C. H., & Khorasanizadeh, S. (2021). Diagnostic yield of advanced genetic testing in patients with hereditary neuropathies: A retrospective single-site study. *Muscle Nerve*, 64(4), 454–461. <https://doi.org/10.1002/mus.27368>
17. Fledrich, R., Mannil, M., Leha, A., Ehbrecht, C., Solari, A., Pelayo-Negro, A. L., Berciano, J., Schlotter-Weigel, B., Schniser, T. J., Prukop, T., Garcia-Angarita, N., Czesnik, D., Haberlová, J., Mazanec, R., Paulus, W., Beissbarth, T., Walter, M. C., Triaal, C., Hogrel, J. Y.,...Sereda, M. W. (2017). Biomarkers predict outcome in Charcot-Marie-Tooth disease 1A. *J Neurol Neurosurg Psychiatry*, 88(11), 941–952. <https://doi.org/10.1136/jnnp-2017-315721>
18. Fridman, V., Bundy, B., Reilly, M. M., Pareyson, D., Bacon, C., Burns, J., Day, J., Feely, S., Finkel, R. S., Grider, T., Kirk, C. A., Herrmann, D. N., Laurá, M., Li, J., Lloyd, T., Sumner, C. J., Muntoni, F., Piscosquito, G., Ramchandren, S.,...Shy, M. E. (2015). CMT subtypes and disease burden in patients enrolled in the Inherited Neuropathies Consortium natural history study: a cross-sectional analysis. *J Neurol Neurosurg Psychiatry*, 86(8), 873–878. <https://doi.org/10.1136/jnnp-2014-308826>

19. Fridman, V., Sillau, S., Acsadi, G., Bacon, C., Dooley, K., Burns, J., Day, J., Feely, S., Finkel, R. S., Grider, T., Gutmann, L., Herrmann, D. N., Kirk, C. A., Knause, S. A., Laura, M., Lewis, R. A., Li, J., Lloyd, T. E., Moroni, I.,...Shy, M. E. (2020). A longitudinal study of CMT1A using Rasch analysis based CMT neuropathy and examination scores. *Neurology*, 94(9), e884-e896. <https://doi.org/10.1212/wnl.0000000000009035>
20. Gantner, M. L., Eade, K., Wallace, M., Handzlik, M. K., Fallon, R., Trombley, J., Bonelli, R., Giles, S., Harkins-Perry, S., Heeren, T. F. C., Sauer, L., Ideguchi, Y., Baldini, M., Schepke, L., Dorrell, M. I., Kitano, M., Hart, B. J., Cai, C., Nagasaki, T.,...Friedlander, M. (2019). Serine and Lipid Metabolism in Macular Disease and Peripheral Neuropathy. *N Engl J Med*, 381(15), 1422-1433. <https://doi.org/10.1056/NEJMoa1815111>
21. Guan, Y., Zhang, Y., Shen, X. M., Zhou, L., Shang, X., Peng, Y., Hu, Y., & Li, W. (2021). Charcot-Marie-Tooth Disease With Episodic Rhabdomyolysis Due to Two Novel Mutations in the β Subunit of Mitochondrial Trifunctional Protein and Effective Response to Modified Diet Therapy. *Front Neurol*, 12, 694966. <https://doi.org/10.3389/fneur.2021.694966>
22. Hackett, A. R., Strickland, A., & Milbrandt, J. (2020). Disrupting insulin signaling in Schwann cells impairs myelination and induces a sensory neuropathy. *Glia*, 68(5), 963–978. <https://doi.org/10.1002/glia.23755>
23. Handzlik, M. K., Gengatharan, J. M., Frizzi, K. E., McGregor, G. H., Martino, C., Rahman, G., Gonzalez, A., Moreno, A. M., Green, C. R., Guernsey, L. S., Lin, T., Tseng, P., Ideguchi, Y., Fallon, R. J., Chaix, A., Panda, S., Mali, P., Wallace, M., Knight, R.,...Metallo, C. M. (2023). Insulin-regulated serine and lipid metabolism drive peripheral neuropathy. *Nature*, 614(7946), 118–124. <https://doi.org/10.1038/s41586-022-05637-6>
24. Hori, T., Fukao, T., Kobayashi, H., Teramoto, T., Takayanagi, M., Hasegawa, Y., Yasuno, T., Yamaguchi, S., & Kondo, N. (2010). Carnitine palmitoyltransferase 2 deficiency: the time-course of blood and urinary acylcarnitine levels during initial L-carnitine supplementation. *Tohoku J Exp Med*, 221(3), 191–195. <https://doi.org/10.1620/tjem.221.191>
25. Hsu, W. C., Chiu, S. Y., Yen, A. M., Chen, L. S., Fann, C. Y., Liao, C. S., & Chen, H. H. (2012). Somatic neuropathy is an independent predictor of all- and diabetes-related mortality in type 2 diabetic patients: a population-based 5-year follow-up study (KCIS No. 29). *Eur J Neurol*, 19(9), 1192–1198. <https://doi.org/10.1111/j.1468-1331.2011.03659.x>
26. Hwang, J. W., Pyun, S. B., & Kwon, H. K. (2016). Relationship of Vascular Factors on Electrophysiologic Severity of Diabetic Neuropathy. *Ann Rehabil Med*, 40(1), 56–65. <https://doi.org/10.5535/arm.2016.40.1.56>

27. Jariwal, R., Shoua, B., Sabetian, K., Natarajan, P., & Cobos, E. (2018). Unmasking a Case of Asymptomatic Charcot-Marie-Tooth Disease (CMT1A) With Vincristine. *J Investig Med High Impact Case Rep*, 6, 2324709618758349. <https://doi.org/10.1177/2324709618758349>
28. Khalil, M., Pirpamer, L., Hofer, E., Voortman, M. M., Barro, C., Leppert, D., Benkert, P., Ropele, S., Enzinger, C., Fazekas, F., Schmidt, R., & Kuhle, J. (2020). Serum neurofilament light levels in normal aging and their association with morphologic brain changes. *Nat Commun*, 11(1), 812. <https://doi.org/10.1038/s41467-020-14612-6>
29. Khalil, M., Teunissen, C. E., Otto, M., Piehl, F., Sormani, M. P., Gattringer, T., Barro, C., Kappos, L., Comabella, M., Fazekas, F., Petzold, A., Blennow, K., Zetterberg, H., & Kuhle, J. (2018). Neurofilaments as biomarkers in neurological disorders. *Nat Rev Neurol*, 14(10), 577–589. <https://doi.org/10.1038/s41582-018-0058-z>
30. Kovale, S., Terauda, R., Millere, E., Taurina, G., Murmane, D., Isakova, J., Kenina, V., & Gailite, L. (2021). GJB1 Gene Analysis in Two Extended Families with X-Linked Charcot-Marie-Tooth Disease. *Case Rep Neurol*, 13(2), 422–428. <https://doi.org/10.1159/000515170>
31. Lehmann, R. (2021). From bedside to bench-practical considerations to avoid pre-analytical pitfalls and assess sample quality for high-resolution metabolomics and lipidomics analyses of body fluids. *Anal Bioanal Chem*, 413(22), 5567–5585. <https://doi.org/10.1007/s00216-021-03450-0>
32. Lehotay, D. C., Hall, P., Lepage, J., Eichhorst, J. C., Etter, M. L., & Greenberg, C. R. (2011). LC–MS/MS progress in newborn screening. *Clinical Biochemistry*, 44(1), 21–31. <https://doi.org/10.1016/j.clinbiochem.2010.08.007>
33. Lin, C., Tian, Q., Guo, S., Xie, D., Cai, Y., Wang, Z., Chu, H., Qiu, S., Tang, S., & Zhang, A. (2024). Metabolomics for Clinical Biomarker Discovery and Therapeutic Target Identification. *Molecules*, 29(10). <https://doi.org/10.3390/molecules29102198>
34. Mai, M., Tönjes, A., Kovacs, P., Stumvoll, M., Fiedler, G. M., & Leichtle, A. B. (2013). Serum Levels of Acylcarnitines Are Altered in Prediabetic Conditions. *PLoS One*, 8(12), e82459. <https://doi.org/10.1371/journal.pone.0082459>
35. Mariotto, S., Farinazzo, A., Magliozzi, R., Alberti, D., Monaco, S., & Ferrari, S. (2018). Serum and cerebrospinal neurofilament light chain levels in patients with acquired peripheral neuropathies. *J Peripher Nerv Syst*, 23(3), 174–177. <https://doi.org/10.1111/jns.12279>
36. Millere, E., Rots, D., Simrén, J., Ashton, N. J., Kupats, E., Micule, I., Priedite, V., Kurjane, N., Blennow, K., Gailite, L., Zetterberg, H., & Kenina, V. (2021). Plasma neurofilament light chain as a potential biomarker in Charcot-Marie-Tooth disease. *Eur J Neurol*, 28(3), 974–981. <https://doi.org/10.1111/ene.14689>

37. Morrow, J. M., Evans, M. R. B., Grider, T., Sinclair, C. D. J., Thedens, D., Shah, S., Yousry, T. A., Hanna, M. G., Nopoulos, P., Thornton, J. S., Shy, M. E., & Reilly, M. M. (2018). Validation of MRC Centre MRI calf muscle fat fraction protocol as an outcome measure in CMT1A. *Neurology*, 91(12), e1125-e1129. <https://doi.org/10.1212/wnl.0000000000006214>
38. Morrow, J. M., Sinclair, C. D., Fischmann, A., Machado, P. M., Reilly, M. M., Yousry, T. A., Thornton, J. S., & Hanna, M. G. (2016). MRI biomarker assessment of neuromuscular disease progression: a prospective observational cohort study. *Lancet Neurol*, 15(1), 65–77. [https://doi.org/10.1016/s1474-4422\(15\)00242-2](https://doi.org/10.1016/s1474-4422(15)00242-2)
39. Murphy, S. M., Herrmann, D. N., McDermott, M. P., Scherer, S. S., Shy, M. E., Reilly, M. M., & Pareyson, D. (2011). Reliability of the CMT neuropathy score (second version) in Charcot-Marie-Tooth disease. *J Peripher Nerv Syst*, 16(3), 191–198. <https://doi.org/10.1111/j.1529-8027.2011.00350.x>
40. Noland, R. C., Koves, T. R., Seiler, S. E., Lum, H., Lust, R. M., Ilkayeva, O., Stevens, R. D., Hegardt, F. G., & Muoio, D. M. (2009). Carnitine insufficiency caused by aging and overnutrition compromises mitochondrial performance and metabolic control. *J Biol Chem*, 284(34), 22840–22852. <https://doi.org/10.1074/jbc.M109.032888>
41. Novello, B. J., & Pobre, T. (2025). *Electrodiagnostic Evaluation of Peripheral Neuropathy*. In StatPearls. StatPearls Publishing Copyright © 2025, StatPearls Publishing LLC.
42. Padilha, J. P. D., Brasil, C. S., Hoefel, A. M. L., Winckler, P. B., Donis, K. C., Brusius-Facchin, A. C., & Saute, J. A. M. (2020). Diagnostic yield of targeted sequential and massive panel approaches for inherited neuropathies. *Clin Genet*, 98(2), 185–190. <https://doi.org/10.1111/cge.13793>
43. Pipis, M., Rossor, A. M., Laura, M., & Reilly, M. M. (2019). Next-generation sequencing in Charcot-Marie-Tooth disease: opportunities and challenges. *Nat Rev Neurol*, 15(11), 644–656. <https://doi.org/10.1038/s41582-019-0254-5>
44. Ramchandren, S. (2017). Charcot-Marie-Tooth Disease and Other Genetic Polyneuropathies. *Continuum (Minneapolis, Minn)*, 23(5, *Peripheral Nerve and Motor Neuron Disorders*), 1360–1377. <https://doi.org/10.1212/con.0000000000000529>
45. Reuter, S. E., & Evans, A. M. (2012). Carnitine and acylcarnitines: pharmacokinetic, pharmacological and clinical aspects. *Clin Pharmacokinet*, 51(9), 553–572. <https://doi.org/10.1007/bf03261931>
46. Richards, S., Aziz, N., Bale, S., Bick, D., Das, S., Gastier-Foster, J., Grody, W. W., Hegde, M., Lyon, E., Spector, E., Voelkerding, K., & Rehm, H. L. (2015). Standards and guidelines for the interpretation of sequence variants: a joint consensus recommendation of the American College of Medical Genetics and Genomics and the Association for Molecular Pathology. *Genet Med*, 17(5), 405–424. <https://doi.org/10.1038/gim.2015.30>

47. Rossor, A. M., Kapoor, M., Wellington, H., Spaulding, E., Sleight, J. N., Burgess, R. W., Laura, M., Zetterberg, H., Bacha, A., Wu, X., Heslegrave, A., Shy, M. E., & Reilly, M. M. (2022). A longitudinal and cross-sectional study of plasma neurofilament light chain concentration in Charcot-Marie-Tooth disease. *J Peripher Nerv Syst*, 27(1), 50–57. <https://doi.org/10.1111/jns.12477>
48. Rossor, A. M., Shy, M. E., & Reilly, M. M. (2020). Are we prepared for clinical trials in Charcot-Marie-Tooth disease? *Brain Res*, 1729, 146625. <https://doi.org/10.1016/j.brainres.2019.146625>
49. Rovite, V., Wolff-Sagi, Y., Zaharenko, L., Nikitina-Zake, L., Grens, E., & Klovins, J. (2018). Genome Database of the Latvian Population (LGDB): Design, Goals, and Primary Results. *J Epidemiol*, 28(8), 353–360. <https://doi.org/10.2188/jea.JE20170079>
50. Rudnik-Schöneborn, S., Tölle, D., Senderek, J., Eggermann, K., Elbracht, M., Kornak, U., von der Hagen, M., Kirschner, J., Leube, B., Müller-Felber, W., Schara, U., von Au, K., Wiczorek, D., Bußmann, C., & Zerres, K. (2016). Diagnostic algorithms in Charcot-Marie-Tooth neuropathies: experiences from a German genetic laboratory on the basis of 1206 index patients. *Clin Genet*, 89(1), 34–43. <https://doi.org/10.1111/cge.12594>
51. Sames, L., Moore, A., Arnold, R., & Ekins, S. (2014). Recommendations to enable drug development for inherited neuropathies: Charcot-Marie-Tooth and Giant Axonal Neuropathy. *F1000Res*, 3, 83. <https://doi.org/10.12688/f1000research.3751.2>
52. Sandelius, Å., Zetterberg, H., Blennow, K., Adiutori, R., Malaspina, A., Laura, M., Reilly, M. M., & Rossor, A. M. (2018). Plasma neurofilament light chain concentration in the inherited peripheral neuropathies. *Neurology*, 90(6), e518–e524. <https://doi.org/10.1212/wnl.0000000000004932>
53. Saporta, A. S., Sottile, S. L., Miller, L. J., Feely, S. M., Siskind, C. E., & Shy, M. E. (2011). Charcot-Marie-Tooth disease subtypes and genetic testing strategies. *Ann Neurol*, 69(1), 22–33. <https://doi.org/10.1002/ana.22166>
54. Sarmad, S., Viant, M. R., Dunn, W. B., Goodacre, R., Wilson, I. D., Chappell, K. E., Griffin, J. L., O'Donnell, V. B., Naicker, B., Lewis, M. R., & Suzuki, T. (2023). A proposed framework to evaluate the quality and reliability of targeted metabolomics assays from the UK Consortium on Metabolic Phenotyping (MAP/UK). *Nat Protoc*, 18(4), 1017–1027. <https://doi.org/10.1038/s41596-022-00801-8>
55. Sens, A., Rischke, S., Hahnefeld, L., Dorochow, E., Schäfer, S. M. G., Thomas, D., Köhm, M., Geisslinger, G., Behrens, F., & Gurke, R. (2023). Pre-analytical sample handling standardization for reliable measurement of metabolites and lipids in LC–MS-based clinical research. *J Mass Spectrom Adv Clin Lab*, 28, 35–46. <https://doi.org/10.1016/j.jmsacl.2023.02.002>
56. Shao, M. M., Xiang, H. J., Lu, H., Yin, P. H., Li, G. W., Wang, Y. M., Chen, L., Chen, Q. G., Zhao, C., Lu, Q., Wu, T., & Ji, G. (2022). Candidate metabolite markers of peripheral neuropathy in Chinese patients with type 2 diabetes. *Am J Transl Res*, 14(8), 5420–5440.

57. Shy, M. E., Blake, J., Krajewski, K., Fuerst, D. R., Laura, M., Hahn, A. F., Li, J., Lewis, R. A., & Reilly, M. (2005). Reliability and validity of the CMT neuropathy score as a measure of disability. *Neurology*, 64(7), 1209–1214. <https://doi.org/10.1212/01.Wnl.0000156517.00615.A3>
58. Soldevilla, B., Cuevas-Martín, C., Ibáñez, C., Santacatterina, F., Alberti, M. A., Simó, C., Casanovas, C., Márquez-Infante, C., Sevilla, T., Pascual, S. I., Sánchez-Aragó, M., Espinos, C., Palau, F., & Cuezva, J. M. (2017). Plasma metabolome and skin proteins in Charcot-Marie-Tooth 1A patients. *PLoS One*, 12(6), e0178376. <https://doi.org/10.1371/journal.pone.0178376>
59. Steiner, N., Müller, U., Hajek, R., Sevcikova, S., Borjan, B., Jöhrer, K., Göbel, G., Pircher, A., & Günsilius, E. (2018). The metabolomic plasma profile of myeloma patients is considerably different from healthy subjects and reveals potential new therapeutic targets. *PLoS One*, 13(8), e0202045. <https://doi.org/10.1371/journal.pone.0202045>
60. Takaya, H., Namisaki, T., Kitade, M., Shimozaoto, N., Kaji, K., Tsuji, Y., Nakanishi, K., Noguchi, R., Fujinaga, Y., Sawada, Y., Saikawa, S., Sato, S., Kawaratani, H., Moriya, K., Akahane, T., & Yoshiji, H. (2019). Acylcarnitine: Useful biomarker for early diagnosis of hepatocellular carcinoma in non-steatohepatitis patients. *World J Gastrointest Oncol*, 11(10), 887-897. <https://doi.org/10.4251/wjgo.v11.i10.887>
61. Thachil, A., Wang, L., Mandal, R., Wishart, D., & Blydt-Hansen, T. (2024). An Overview of Pre-Analytical Factors Impacting Metabolomics Analyses of Blood Samples. *Metabolites*, 14(9). <https://doi.org/10.3390/metabo14090474>
62. Ueland, T., Svardal, A., Øie, E., Askevold, E. T., Nymoen, S. H., Bjørndal, B., Dahl, C. P., Gullestad, L., Berge, R. K., & Aukrust, P. (2013). Disturbed carnitine regulation in chronic heart failure--increased plasma levels of palmitoyl-carnitine are associated with poor prognosis. *Int J Cardiol*, 167(5), 1892–1899. <https://doi.org/10.1016/j.ijcard.2012.04.150>
63. Vaeth, S., Andersen, H., Christensen, R., & Jensen, U. B. (2021). A Search for Undiagnosed Charcot-Marie-Tooth Disease Among Patients Registered with Unspecified Polyneuropathy in the Danish National Patient Registry. *Clin Epidemiol*, 13, 113–120. <https://doi.org/10.2147/cep.S292676>
64. Viader, A., Sasaki, Y., Kim, S., Strickland, A., Workman, C. S., Yang, K., Gross, R. W., & Milbrandt, J. (2013). Aberrant Schwann cell lipid metabolism linked to mitochondrial deficits leads to axon degeneration and neuropathy. *Neuron*, 77(5), 886–898. <https://doi.org/10.1016/j.neuron.2013.01.012>
65. Yuan, A., Rao, M. V., Veeranna, & Nixon, R. A. (2017). Neurofilaments and Neurofilament Proteins in Health and Disease. *Cold Spring Harb Perspect Biol*, 9(4). <https://doi.org/10.1101/cshperspect.a018309>
66. Zhang, H., Zhou, Z. W., & Sun, L. (2021). Aminoacyl-tRNA synthetases in Charcot-Marie-Tooth disease: A gain or a loss? *J Neurochem*, 157(3), 351–369. <https://doi.org/10.1111/jnc.15249>

67. Zhao, J., Zhu, Y., Hyun, N., Zeng, D., Uppal, K., Tran, V. T., Yu, T., Jones, D., He, J., Lee, E. T., & Howard, B. V. (2015). Novel metabolic markers for the risk of diabetes development in American Indians. *Diabetes Care*, 38(2), 220–227. <https://doi.org/10.2337/dc14-2033>
68. Zhu, C., Liang, Q. L., Hu, P., Wang, Y. M., & Luo, G. A. (2011). Phospholipidomic identification of potential plasma biomarkers associated with type 2 diabetes mellitus and diabetic nephropathy. *Talanta*, 85(4), 1711–1720. <https://doi.org/10.1016/j.talanta.2011.05.036>
69. Zordoky, B. N., Sung, M. M., Ezekowitz, J., Mandal, R., Han, B., Bjorndahl, T. C., Bouatra, S., Anderson, T., Oudit, G. Y., Wishart, D. S., & Dyck, J. R. (2015). Metabolomic fingerprint of heart failure with preserved ejection fraction. *PLoS One*, 10(5), e0124844. <https://doi.org/10.1371/journal.pone.0124844>

Acknowledgements

I would like to express my deepest gratitude to my scientific advisor, Associate Professor Viktorija Kēniņa, primarily for her skilled guidance and motivation throughout the development of this Thesis. Thank you for your time, invaluable support, and significant contribution to the completion of this work.

I would also like to sincerely thank my scientific consultant, Associate Professor Kristaps Kļaviņš. With his support, insightful comments, and constructive suggestions, the progress of this work was significantly accelerated and improved.

My appreciation also goes to all the doctors and residents who assisted during the research process. I would like to extend a special thank you to Dmitrijs Rots, Marija Jurčenko, and Arta Grosmane. I am also grateful to senior researcher Linda Gailīte for her support in preparing the publications, and to Miķelis Bendiks for providing me with a space to spend long hours writing this Thesis.

Finally, I wish to express my heartfelt thanks to my entire family for their unwavering support, strength, and patience throughout my doctoral studies. Special thanks to my husband Kaspars and my daughters Nora and Hilda.

Annexes

Statement from the Central Medical Ethics Committee

Centrālā medicīnas ētikas komiteja

Brīvības iela 72, Rīga, LV-1011 • Tālr. 67876182 • Fakss 67876071 • E-pasts: vm@vm.gov.lv

Rīgā

21.03.2018. Nr.3/18-03-21

Rīgas Stradiņa universitātes
Molekulārās Ģenētikas Zinātniskajai laboratorijai

*Atzinums par pētījumu
„Pārmantoto neiromuskulāro
slimību ģenētiskā analīze”*

Centrālā medicīnas ētikas komiteja 2017.gada 23.novembrī ir izskatījusi Rīgas Stradiņa Universitātes Molekulārās Ģenētikas Zinātniskās laboratorijas iesniegto pētījumu „Pārmantoto neiromuskulāro slimību ģenētiskā analīze”.

Pamatojoties uz Centrālās medicīnas ētikas komitejas 2017.gada 23.novembra sēdes protokola Nr.2017-4 punktu Nr.1 un iesniegtajiem labojumiem, tiek izsniegts atzinums, ka Rīgas Stradiņa Universitātes Molekulārās Ģenētikas Zinātniskās laboratorijas pētījums „Pārmantoto neiromuskulāro slimību ģenētiskā analīze” nav pretrunā ar bioētikas normām.

Centrālās medicīnas ētikas
komitejas priekšsēdētājs



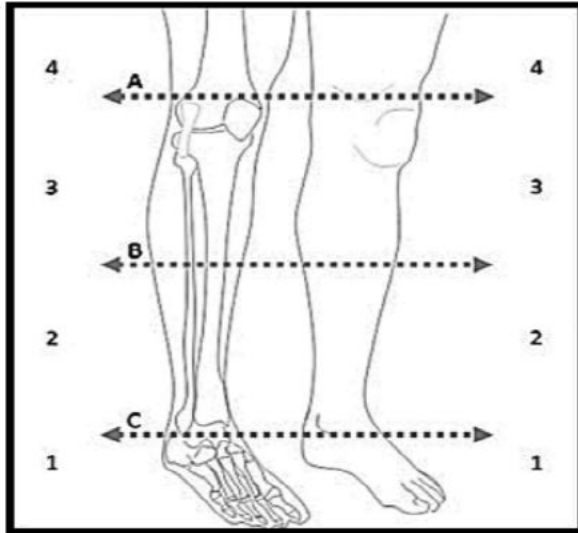
V.Silis

Strautiņš, 67876190
Edgars.Strautins@vm.gov.lv

CMT Neuropathy Score, version 2

Parameter	0	1	2	3	4
Sensory symptoms *	None	Symptoms below or at ankle bones	Symptoms up to the distal half of the calf	Symptoms up to the proximal half of the calf, including knee	Symptoms above knee (above the top of the patella)
Motor symptoms (legs) †	None	Trips, catches toes, slaps feet Shoe inserts	Ankle support or stabilization (AFOs) Foot surgery ‡	Walking aids (cane, walker)	Wheelchair
Motor symptoms (arms)	None	Mild difficulty with buttons	Severe difficulty or unable to do buttons	Unable to cut most foods	Proximal weakness (affect movements involving the elbow and above)
Pinprick sensibility *§	Normal	Decreased below or at ankle bones	Decreased up to the distal half of the calf	Decreased up to the proximal half of the calf, Including knee	Decreased above knee (above the top of the patella)
Vibration/	Normal	Reduced at great toe	Reduced at ankle	Reduced at knee (tibial tuberosity)	Absent at knee and ankle
Strength (legs) ¶	Normal	4+, 4, or 4- on foot dorsiflexion or plantar flexion	≤3 on foot dorsiflexion or ≤3 on foot plantar flexion	≤3 on foot dorsiflexion and ≤3 on plantar flexion	Proximal weakness
Strength (arms) ¶	Normal	4+, 4, or 4- on intrinsic hand muscles **	≤3 on intrinsic Hand muscles **	≤5 on wrist extensors	Weak above elbow
Ulnar CMAP	≥6 mV	4-5.9 mV	2-3.9 mV	0.1-1.9 mV	Absent
(median)	(≥4 mV)	(2.8-3.9)	(1.2-2.7)	(0.1-1.1)	(absent)
Radial SAP amplitude, antidromic testing	≥15 µV	10-14.9 µV	5-9.9 µV	1-4.9 µV	<1 µV

AFO – ankle foot orthoses; CMAP – compound muscle action potential;
SAP – sensory action potential.



- ¹ Use the picture above to discriminate the level of symptoms.
- ² Uses aid most of the time. The patient was prescribed to wear / use or should be wearing the aid in the examiner's opinion.
- ³ See indications for eligible foot surgery.
- ⁴ Abnormal if patient says it is definitely decreased compared to a normal reference point.
- ⁵ Use *Rydel-Seiffer* tuning fork. Defined normal ≥ 5 .
- ⁶ Limb scores refer to MRC grade.
- ⁷ Intrinsic hand muscles strength assessment: test only abductor pollicis brevis (APB) and first dorsal interosseous (FDI), then choose the strongest.

Gened included in exome sequencing

DCAF8; GLE1; ZFYVE26; TBK1; ZFYVE27; TFG; CLP1; SCN11A; AP1S1; MPV17; PRKCG; UNC13A; PDYN; SOX10; SLC5A7; SCN10A; SCO2; MAP1B; HMBS; FDX2; OPTN; GNE; MTMR2; COL13A1; DHH; XPA; PRDM12; AAAS; PLA2G6; SLC5A2; SLC5A3; GJC2; TTPA; PIP5K1C; ABCA1; DNAH10; HACE1; JAG1; PMM2; ERLIN1; TRIP4; ERLIN2; L1CAM; SETX; FA2H; GJB1; LAS1L; GJB3; TDP1; PAH; CDK16; LRSAM1; HEXB; HEXA; LITAF; LYST; FARS2; AIFM1; TRIM2; RARS; FLVCR1; NEFL; TK2; NEFH; SLC18A3; MYBPC1; ELOVL4; ELOVL5; ARG1; KCND3; NIPA1; TIMM22; TMEM173; FAM126A; HADHB; HADHA; MED25; INF2; MYOT; PTRH2; VAMP1; PMP2; GARS; L2HGDH; ASAH1; GRN; CTDPL1; AP5Z1; ATL3; WDR45B; ATL1; ATL2; KCNA2; PRUNE1; *C1orf194*; HOXD10; FGD4; CHRND; CHRNG; TMEM65; CHRNE; MFN2; ZNF106; HARS; GSN; KIDINS220; ELP1; TUBB4A; FIG4; PLP1; UBAP1; COQ8A; AGRN; RPH3A; ABHD12; NAGLU; TUBB3; CHP1; NEK1; SLC25A42; SLC16A2; MTPAP; SLC25A46; NKX6-2; DGAT2; PCYT2; AGTPBP1; GPT2; VRK1; TUBA4A; BSCL2; MAG; STIM1; SQSTM1; RNASEH2B; DNMT1; ITPR3; ATXN2; KLC2; BAG3; PSAP; CLTCL1; RNF170; AP4S1; SMN1; TIA1; FUS; WFS1; FBXO38; GFPT1; REEP1; DMXL2; REEP2; SLC25A1; SNAP25; CNTNAP1; PTEN; BICD2; AP4M1; ATP7B; OPA1; SPR; OPA3; EMILIN1; SERAC1; ATP7A; SPG11; SNAP29; COA7; DST; PLEKHG5; SIGMAR1; VPS13A; SORD; APOA1; VPS37A; NGF; COASY; DNAJC3; SLC25A15; NEMF; RRM2B; SLC25A19; ANG; AGXT; SLC25A4; FXN; *C9orf72*; PRPS1; LRP4; DNAJB2; TTR; MSTO1; DNAJB5; SH3BP4; IARS2; HNRNPA1; UBQLN2; NTRK1; MGME1; KCNJ10; TRPA1; ASCC1; AHNK2; DDHD2; NAGA; PTPN11; DDHD1; MCM3AP; SUCLA2; POLR3A; VAPB; MYO1A; STUB1; MMACHC; SPG21; ARL6IP1; PRF1; NUDT2; GBA2; EDNRB; FLAD1; PIEZO2; PDK3; SLC12A6; SIL1; *C12orf65*; ARSA; ENTPD1; MUSK; ALG6; IFRD1; ALG2; CPT1C; CYP27A1; AFG3L2; BTBD; CYP2U1; KARS; SUCLG1; DNA2; PFN1; SPTBN4; MTTT; PIK3R5; DGUOK; SGPL1; SPAST; MICAL1; B4GALNT1; SURF1; EGR2; XRCC4; SLC33A1; XRCC1; PRG4; NOTCH2NLC; SPART; AIMP1; TH; WNK1; NDUFAF5; ATM; ALDH18A1; RETREG1; TECPR2; FBXL4; AARS; FASTKD2; GBE1; AP4E1; SIPA1L2; UCHL1; HINT1; SPTLC1; SPTLC2; SPTLC3; PRX; KIF1C; KIF1B; KIF1A; SPTAN1; WARS; MME; MRPS25; TOP3A; AMPD2; CYP7B1; GAN; TNNT2; MAPT; RAPSN; RAB7A; IGHMBP2; HSD17B4; IBA57; TYMP; DRP2; LMNA; EXOSC8; CD59; EXOSC3; CCT5; DYNC1H1; GCH1; GBF1; PEX10; PEX12; FAH; *C19orf12*; MYO9A; APTX; COLQ; XK; KIF26B; MARS; CTNBN1; PNPLA6; TARDBP; SCARB2; DPAGT1; WASHC5; CPOX; COX6A1; COX6A2; YARS2; MPZ; SCN9A; KIF5A; SACS; CAPN1; SBF1; SBF2; CHRNB1; PHYH; PUS1; ALG14; ANXA11; ATAD3A; ALDH3A2; PREPL; POLG2; SCN8A; DOK7; TBC1D24; MATR3; CHRNA1; RTN2; VCP; UBA5; CHAT; SLC1A4; KLHL13; NDRG1; TOR1AIP1; FBLN5; CACNA1G; RNASEH1; MYH14; MORC2; COX10; PRPH; YARS; PRNP; DARS; SMAD3; PDHA1; SYT2; ZFH2; SLC52A2; SLC52A3; CHCHD10; COQ9; AP4B1; COQ7; PHOX2B; COQ6; COQ4; COQ2; GCLC; AMACR; TRPV4; CHMP2B; TBCE; GNB4; UBA1; DEGS1; COX20; KDM5C; HSPB8; NGLY1; SLC2A1; HSPB1; ADAR; LDB3; HSPB3; GRM1; DHTKD1; HK1; IRF2BPL; GMPPB; SEPT9; GMPPA; RBM7; ABCD1; SCYL1; POLG; ARHGEF10; MARS2; BCKDHB; TWNK; DARS2; PEX1; DNMT2; PEX7; ALS2; ACOX1; SCN4A; PLEC; LAMA5; DCTN2; DCTN1; PNKP; ETFDH; SPG7; ATP1A1; PPOX; NT5C2; CLCN2; HSPD1; ERBB3; SH3TC2; ERBB4; LRIG3; LAMB2; GDAP1; SOD1; RPLA; GALT; PMP22; ERCC8; ATP13A2; ERCC6; GLA.

**Plasma metabolites identified in plasma samples from
CMT patients and the control group**

Metabolites	4-Hydroxyproline
	Butyrylcarnitine
	Carnitine
	Citrulline
	Creatinine
	Glycine
	Isovalerylcarnitine
	Kynurenine
	L-Acetylcarnitine
	L-Alanine
	L-Arginine
	L-Asparagine
	L-Aspartic Acid
	L-Cystine
	L-Glutamic Acid
	L-Glutamine
	L-Histidine
	L-Leucine
	L-Isoleucine
	L-Lysine
	L-Methionine
	L-Octanoylcarnitine
	L-Phenylalanine
	L-Proline
	L-Serine
	L-Threonine
	L-Tryptophan
	L-Tyrosine
	L-Valine
	Methylhistidine
	Ornithine
	Propionylcarnitine
	Taurine